QEX

September/October 2022

www.arrl.org

A Forum for Communications Experimenters

Issue No. 334

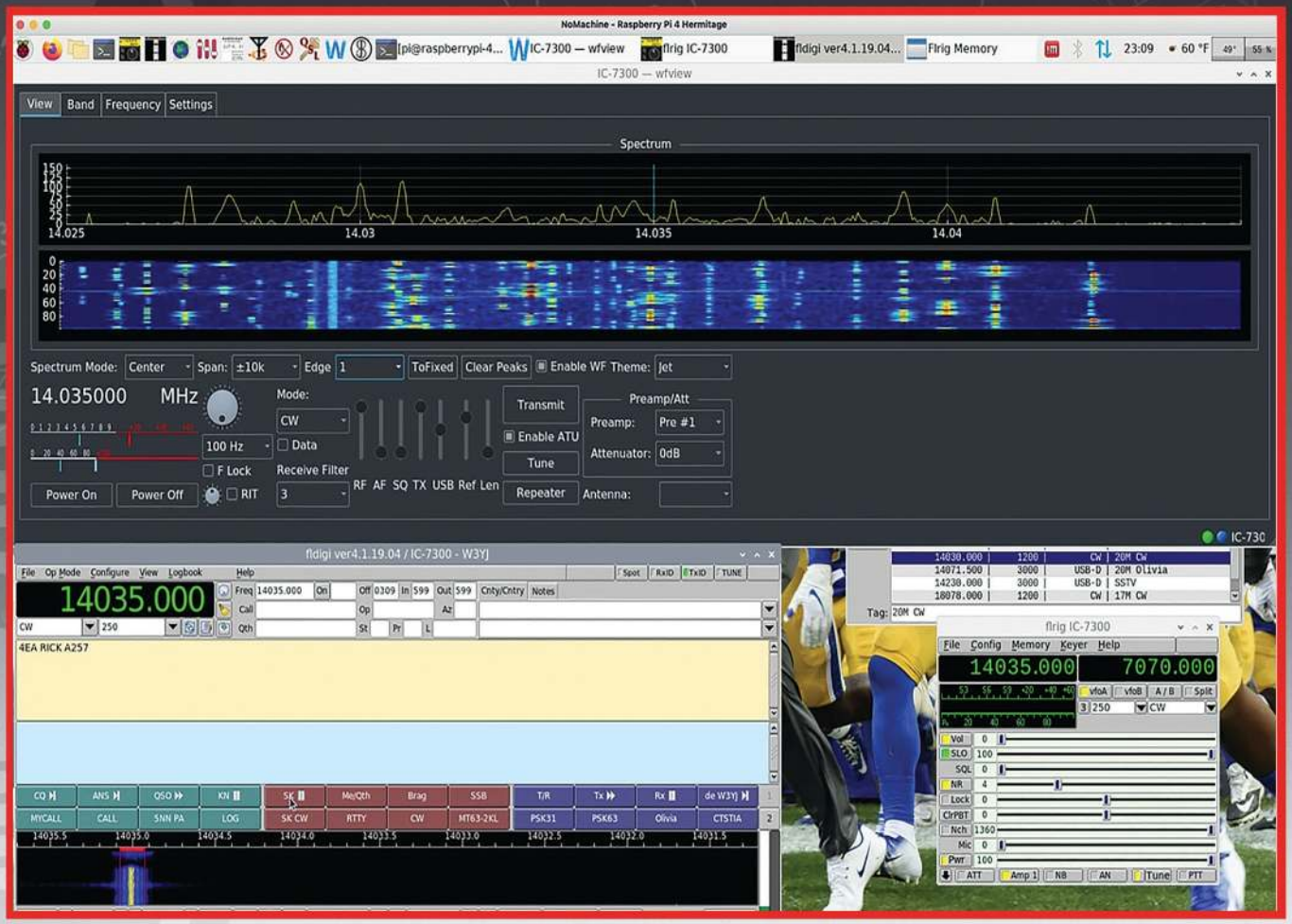

W3YJ shows full screen full color waterfall displays on an external monitor.

The entire Amateur Radio family at KENWOOD would like to express our sincerest and deepest appreciation for everything Bob Bruninga brought to the Amateur Radio world. We have shared some wonderful and memorable times and will always cherish the support and friendship Bob shared with us.

Akira Suzuki
Director of the Board
Senior Managing Executive Officer
COO Public Service Sector
JVCKENWOOD Corporation

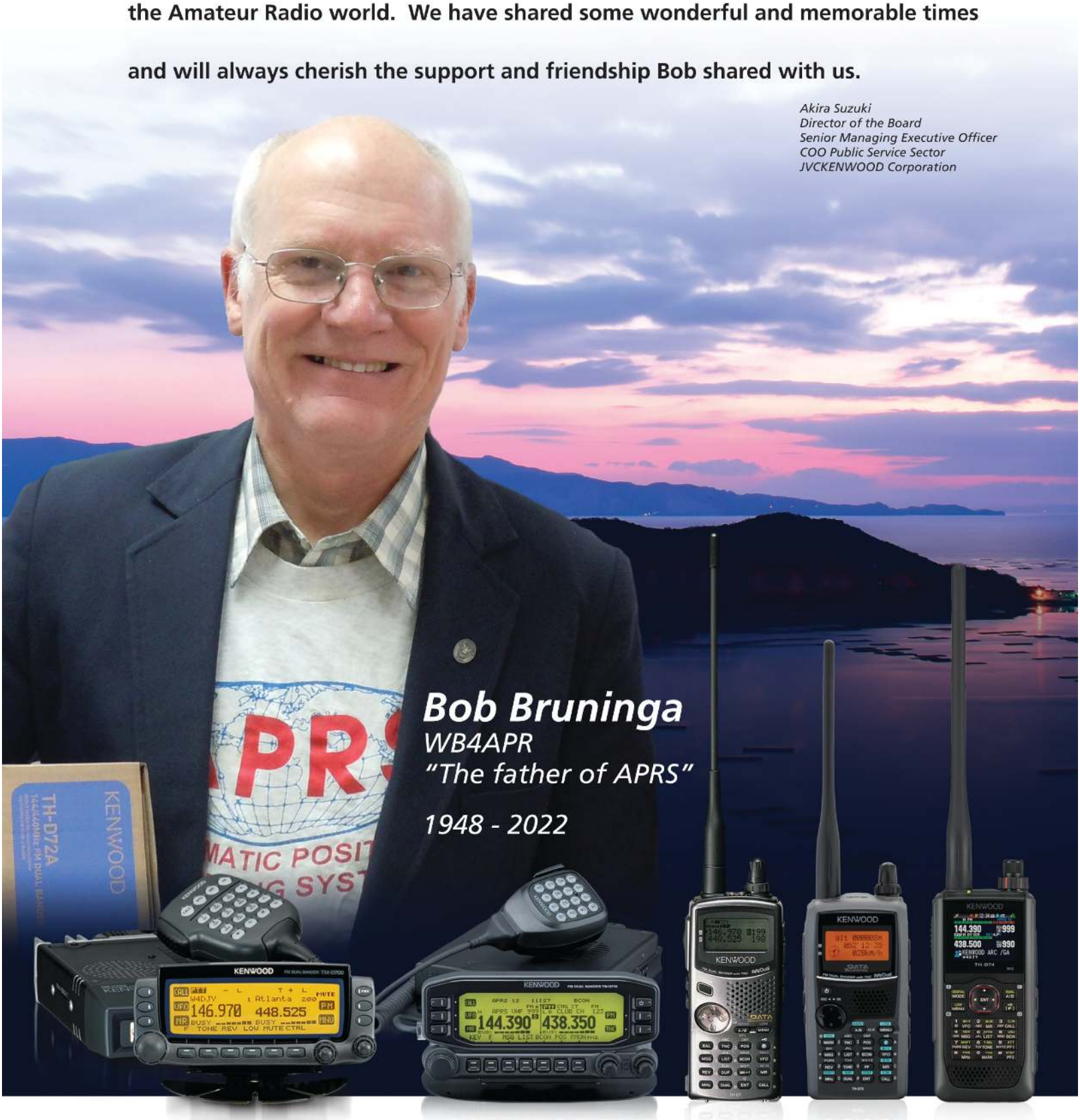

KENWOOD

Customer Support/Distribution Customer Support:
(310) 639-4200 Fax: (310) 537-8235 **www.kenwood.com/usa**
ADS#06022

QEX (ISSN: 0886-8093) is published bimonthly in January, March, May, July, September, and November by the American Radio Relay League, 225 Main St., Newington, CT 06111-1400. Periodicals postage paid at Hartford, CT and at additional mailing offices.

POSTMASTER: Send address changes to: QEX, 225 Main St., Newington, CT 06111-1400
Issue No. 334

Publisher
American Radio Relay League

Kazimierz "Kai" Siwiak, KE4PT
Editor

Lori Weinberg, KB1EIB
Assistant Editor

Scotty Cowling, WA2DFI
Ray Mack, W5IFS
Contributing Editors

Production Department

Becky R. Schoenfeld, W1BXY
Director of Publications and Editorial

Michelle Bloom, WB1ENT
Production Supervisor

David Pingree, N1NAS
Senior Technical Illustrator

Brian Washing
Technical Illustrator

Advertising Information

Janet L. Rocco, W1JLR
Business Services
860-594-0203 – Direct
800-243-7768 – ARRL
860-594-4285 – Fax

Circulation Department

Cathy Stepina
QEX Circulation

Offices

225 Main St., Newington, CT 06111-1400 USA
Telephone: 860-594-0200
Fax: 860-594-0259 (24-hour direct line)
Email: **qex@arrl.org**

Subscription rate for 6 print issues:

In the US: $29

US by First Class Mail: $40;

International and Canada by Airmail: $35

ARRL members receive the digital edition of *QEX* as a member benefit.

In order to ensure prompt delivery, we ask that you periodically check the address information on your mailing label. If you find any inaccuracies, please contact the Circulation Department immediately. Thank you for your assistance.

September/October 2022

About the Cover

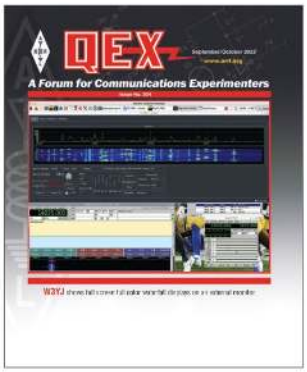

Harry Bloomberg, W3YJ, describes how to use wfview software to display the waterfall of late-model Icom radios on your desktop monitor. The software provides a growing list of rig-control features like tuning, setting audio levels, and changing modes. For radios that can connect to a network, you can use a network connection instead of a USB cable. There are many ways of configuring your waterfall display, including expanding it to cover your entire desktop. You can also select from many different color schemes, as well as select the bandwidth that will be displayed. Double-clicking on a signal of interest will automatically retune your radio, and place that signal in the middle of your pass band. With wfview you can have an external waterfall displayed on a nice large monitor in your station.

In This Issue

Index of Advertisers

The American Radio Relay League

The American Radio Relay League, Inc., is a noncommercial association of radio amateurs, organized for the promotion of interest in Amateur Radio communication and experimentation, for the establishment of networks to provide communications in the event of disasters or other emergencies, for the advancement of the radio art and of the public welfare, for the representation of the radio amateur in legislative matters, and for the maintenance of fraternalism and a high standard of conduct.

ARRL is an incorporated association without capital stock chartered under the laws of the state of Connecticut, and is an exempt organization under Section 501(c)(3) of the Internal Revenue Code of 1986. Its affairs are governed by a Board of Directors, whose voting members are elected every three years by the general membership. The officers are elected or appointed by the Directors. The League is noncommercial, and no one who could gain financially from the shaping of its affairs is eligible for membership on its Board.

"Of, by, and for the radio amateur," ARRL numbers within its ranks the vast majority of active amateurs in the nation and has a proud history of achievement as the standard-bearer in amateur affairs.

A *bona fide* interest in Amateur Radio is the only essential qualification of membership; an Amateur Radio license is not a prerequisite, although full voting membership is granted only to licensed amateurs in the US.

Membership inquiries and general correspondence should be addressed to the administrative headquarters:

ARRL
225 Main St.
Newington, CT 06111 USA
Telephone: 860-594-0200
FAX: 860-594-0259 (24-hour direct line)

Officers

President: Rick Roderick, K5UR
P.O. Box 1463, Little Rock, AR 72203

The purpose of *QEX* is to:

1) provide a medium for the exchange of ideas and information among Amateur Radio experimenters,

2) document advanced technical work in the Amateur Radio field, and

3) support efforts to advance the state of the Amateur Radio art.

All correspondence concerning *QEX* should be addressed to the American Radio Relay League, 225 Main St., Newington, CT 06111 USA. Envelopes containing manuscripts and letters for publication in *QEX* should be marked Editor, *QEX*.

Both theoretical and practical technical articles are welcomed. Manuscripts should be submitted in word-processor format, if possible. We can redraw any figures as long as their content is clear. Photos should be glossy, color or black-and-white prints of at least the size they are to appear in *QEX* or high-resolution digital images (300 dots per inch or higher at the printed size). Further information for authors can be found on the Web at **www.arrl.org/qex/** or by e-mail to **qex@arrl.org**.

Any opinions expressed in *QEX* are those of the authors, not necessarily those of the Editor or the League. While we strive to ensure all material is technically correct, authors are expected to defend their own assertions. Products mentioned are included for your information only; no endorsement is implied. Readers are cautioned to verify the availability of products before sending money to vendors.

Kazimierz "Kai" Siwiak, KE4PT

Perspectives

Keep Talking

In the July/August *Perspectives* I mentioned traditional CW, RTTY and PSK31 as examples of key and keyboard modes that can support conversations on the HF bands rather than just rapid fire minimalist exchanges of modes like FT8.

The column resonated with several hams. Most notably Donald S. Brant Jr., N2VGU, was quick to remind me of the JS8 conversational mode in the JS8Call application by Jordan Sherer, KN4CRD. JS8 is indeed a clever mode implemented in the JS8Call application, and it encourages conversations and rag chewing activity over weak signal paths. JS8Call was brought to the attention of *QST* readers by Steve Ford, WB8IMY, in his "Eclectic Technology" *QST* columns of January 2019 and May 2022. Steve notes that the JS8Call application was built upon the open source WSJT-X software framework, and it employs many aspects of FT8, but it uses the mode in a way that can support keyboard-to-keyboard conversations. It brings the highly popular FT8 technology to the conversationalist.

Our rules and regulations are designed to provide an amateur radio service having fundamental purposes that include the continuation and extension of our unique ability to enhance international goodwill, and to advance skills in both the communication and technical phases of the art. Good ideas, like FT8, can spawn other good ideas, like JS8, that exemplify the fundamental principles of ham radio. Let's keep talking.

In This Issue:

- Harry Bloomberg, W3YJ, displays a waterfall on a remote station.
- Benjamin Neveu controls an SSB receiver with a smartphone.
- Brian Callahan, AD2BA, reviews the CW Record Protocol.
- H. Lawrence Serra, N6NC, explains enhanced 40 m propagation over the North Pacific.
- John Stanley, K4ERO, verifies the short/open method of measuring S11.
- R. Evans Wetmore, K3VFA, presents satellite path link calculations.
- Eric Nichols, KL7AJ, in his Essay Series, solves parallel complex circuits.

Writing for *QEX*

Please continue to send in full-length *QEX* articles, or share a **Technical Note** of several hundred words in length plus a figure or two. *QEX* is edited by Kazimierz "Kai" Siwiak, KE4PT, (**ksiwiak@arrl.org**) and is published bimonthly. *QEX* is a forum for the free exchange of ideas among communications experimenters. All members can access digital editions of all four ARRL magazines: *QST*, *OTA*, *QEX*, and *NCJ* as a member benefit. The *QEX printed edition* is available at an annual subscription rate (6 issues per year) for members and non-members, see **www.arrl.org/qex**.

Would you like to write for *QEX*? We pay $50 per published page for full articles and *QEX* Technical Notes. Get more information and an Author Guide at **www.arrl.org/qex-author-guide**. If you prefer postal mail, send a business-size self-addressed, stamped (US postage) envelope to: *QEX* Author Guide, c/o Maty Weinberg, ARRL, 225 Main St., Newington, CT 06111.

Very kindest regards,
Kazimierz "Kai" Siwiak, KE4PT
QEX Editor

Harry Bloomberg, W3YJ

201 Delafield Rd., Pittsburgh, PA 15215; **hpb@pitt.edu**

View a Waterfall on Your Remote Station with *wfview*

Display full screen full color waterfall displays using wfview.

In the November/December 2020 edition of *QEX* I describe how to use a Raspberry Pi to remotely operate my IC-7300. This has been highly successful. I've earned DXCC with CW, and digital endorsements with this station. However, I could not use one of the Icom IC-7300's best features: its beautiful and colorful waterfall display. Thanks to a new piece of open source software named *wfview,* I can now view the waterfall and do a whole lot more, see **Figure 1**. It is available for download from **wfview.org** and is released under the GNU General Public License v3.0. It installs and runs on Linux, Windows, and MacOS. I have used it only on Linux.

The primary function of *wfview* is to display the waterfall of late-model Icom radios like the IC-705, IC-7300, IC-7610, IC-R8600, IC-7850/51, and IC-9700 on your desktop monitor. It also provides a growing list of rig-control features like tuning, setting audio levels, and changing modes. In addition, if you have a radio like the IC-7610 or IC-705 that can connect to a network, you can use a network connection instead of a USB cable.

There are many ways you can configure your waterfall display. You can expand it to cover your entire desktop if you like. You can select from many different color schemes, some of which may require a trip to your optometrist. You can also change

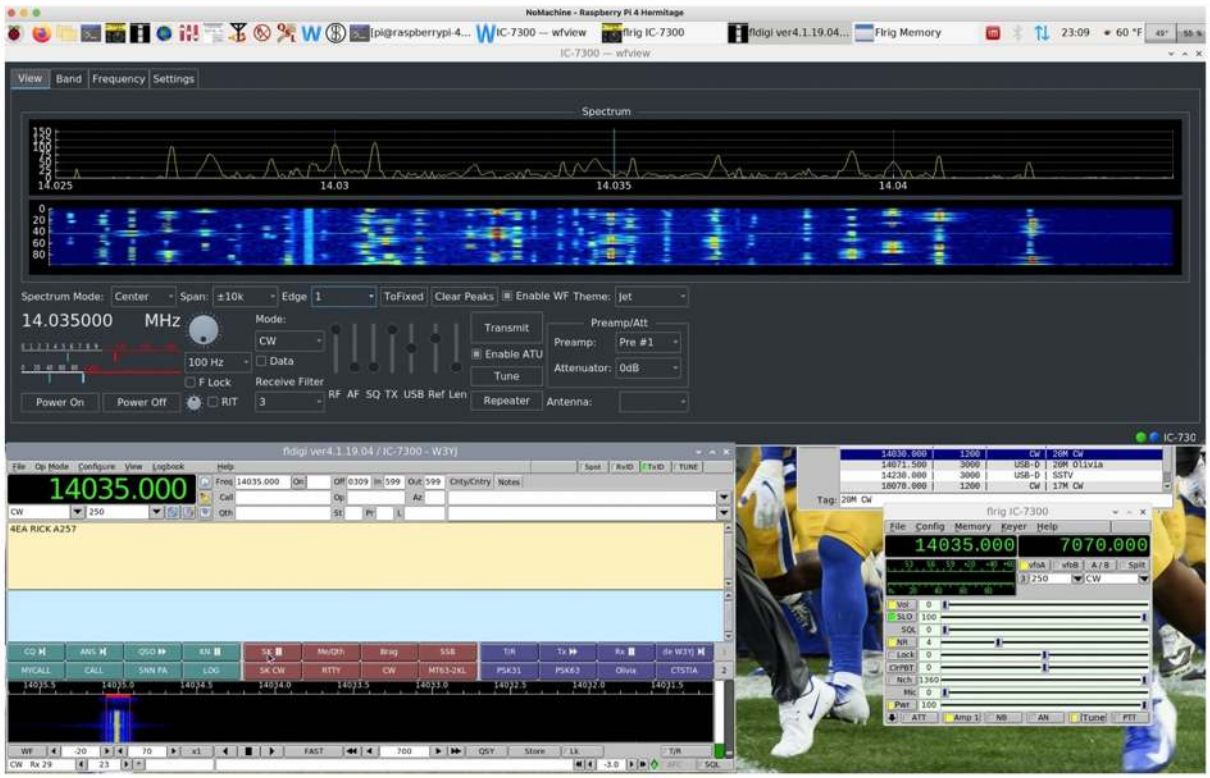

Figure 1 — Screenshot of the desktop of the remote station running *wfview*, and sharing the screen with *Fldigi, and Flrig*.

the bandwidth that will be displayed. If you happen to see a signal of interest in the waterfall, double-clicking on it will automatically retune your radio to place that signal in the middle of your band pass. In some on-line reviews, a few hams have criticized the entry-level IC-7300 for lacking a video port and down-graded the IC-7610 for not using an HDMI connector for external video. With *wfview* you can easily have an external waterfall displayed on a nice large monitor in your station.

In the case of the IC-705, the ability to connect to the built-in wireless RS-BA1 server is more than a convenience. The IC-705 is a wonderful radio, but it is notorious for RFI from a USB cable. With *wfview* I operate my IC-705 completely untethered, which is liberating, simplifies setup, and completely eliminates noise from the USB cable. I use Fldigi in CW mode to key my IC-705 through the wireless connection, so I don't even need an external CW keyer. Yes, when I operate my IC-705 the radio is right in front of me where I can see its waterfall, but it's great to see that waterfall full screen on the 11.6 inch display of the computer I use for portable operation. I use Ubuntu Linux, which provides virtual desktops. It takes just one keystroke to switch from *wfview* to, say, WSJT-X or Fldigi.

Wfview interoperates well with other popular open source software packages like WSJT-X, Fldigi, and Flrig. Even though *wfview* talks directly to your radio, it does not tie up either the virtual or physical USB connection and makes it easy to share the connection with other programs. In Linux, this is done by creating a pointer to the USB connection in your home directory. For Windows, you can install a virtual USB cable.

Likewise, *wfview* allows sharing soundcards. If you're using a physical USB cable, you use the same soundcard devices you've always used. If using a network connection with Linux, the developers have provided a procedure for creating loopback audio devices for your applications like WSJT-X and Fldigi. On Windows, you must install virtual connectors to physical soundcards.

Wfview is a multi-threaded object-oriented program written in C++. The code is written to be cross-platform across Linux, Windows, and MacOS and makes good use of the *qt* toolkit and *QCustomPlot*. Although rig control code is designed to work with almost any Icom radio going back 30 years, it will work best with newer radios. For example, the program has been tested with the IC-718, although as with other older radios, you get only rig control and not the nice waterfall display. The user manual has an entire section titled "Using Older Radios" and contains a detailed matrix of what works on which radios.

Documentation for *wfview* is excellent. It is clearly written, and unlike a lot of documentation for open source projects, it does not assume you're a life-long Linux sysadmin. I followed the provided installation directions and *wfview* installed very easily and without any drama the first time. Support is provided through an on-line forum.

Accessibility for the visually impaired has been considered in designing the program. Although the program is designed to be used with touch screens or a mouse, the entire program can be run from a keyboard with every operation available by keystroke, including one to activate the build-in IC-7300 speech synthesizer. Many common tasks can be performed by pressing just a single key. Tooltips are screen reader compatible.

There are many advanced features in *wfview* I've not yet tried. One is the ability to stream audio using *wfview* connected to your radio as a server to another *wfview* instance through a network as a client. You can also use *wfview* as a wireless server for a radio that does not have a network connection like the IC-7300.

On the *wfview* roadmaps are new core features support for more radios, client-side DSP functions, the ability to assist satellite operation, additional radio controls in separate windows, an emulated HamLib control server, Raspberry Pi GPIO integration for peripherals and radios without CAT commands, enhanced program-to-program communications, and more.

Key to the success of *wfview* development is working as a team and the principles behind open source software. The developers and thousands of world-wide users collaborate in ways that would not be possible had the project been closed source. Everybody gets to share in contributing ideas, working on bug fixes, and suggesting enhancements. Amateur radio really needs to embrace the concept of source code being like a schematic. The programs we use ought to come with source code and support multiple operating systems. *Wfview* is developed by volunteers Elliott Liggett, W6EL (lead developer); Jim Nijkamp, PA8E; Phil Taylor, MØVSE; and Roeland Jansen, PA3MET.

Harry Bloomberg, W3YJ, was first licensed in 1972 as WN3TBL. He recently retired after working many years as a software engineer. Harry graduated from the University of Pittsburgh in 1979 with a BSEE degree. He also holds a Masters of Mathematical Sciences degree from the University of Texas at Dallas. Harry is an alumni member of Panther Amateur Radio Club (PARC) at the University of Pittsburgh. He also belongs to Mercer County ARC and Skyview Radio Society. Harry enjoys CW contesting and working many digital modes. He has had three articles published in QST about NBEMS and wrote a chapter in the ARRL Public Service Communications Handbook *on NBEMS.*

R. Evans Wetmore, K3VFA

1609 Fifth St., Manhattan Beach, CA 90266; **evansw@me.com**

Satellite Link Calculations

Satellite link data includes gain-to-temperature ratio and effective isotropically radiated power.

There has been a clear rise in satellite activity, but there has been little about link calculations that can reveal the viability of both satellites and earth stations in making successful communications. These calculations show how good satellites and earth stations need to be for success.

In General

Link calculations are normally done using decibels, which greatly ease the math required. Also, by convention, power levels are normally stated with respect to a watt, *e.g.*, dBW. With amateur satellites allowance must be made for the constantly changing path length and Doppler shift. We will not address that in this article, since these time-varying parameters are different for each satellite/earth station configuration.

As with any communication channel consideration must be made for the received power and for noise. With these parameters, carrier-to-noise may be readily determined.

Received Power

Received power is set by combining transmit power, path loss, and receive and transmit antenna gains. Specifically:

$$P_r = P_t + G_t - L_p + G_r \tag{1}$$

where:

P_t = transmitter power output (dBW)
G_t = transmit antenna gain over isotropic (dBi)
L_p = path loss (dB)
G_r = receive antenna gain over isotropic (dB)
P_r = received power (dBW).

The antenna gains should include any feed line losses. Adding P_t and G_t yields *EIRP* (effective isotropically radiated power) in dBW. This makes **Eq (1)**,

$$P_r = EIRP - L_p + G_r \tag{2}$$

The path loss between two unobstructed antennas is:

$$L_p = 20\log(f) + 20\log(r) + k_p \tag{3}$$

where:

Lp = path loss (in dB)
f = frequency (in MHz)
r = path distance (same units as k_p)
k_p = –27.55 dB if r is in meters.
k_p = –37.87 dB if r is in feet
k_p = 32.45 dB if r is in kilometers
k_p = 36.58 dB if r is in statute miles.

Noise

Using linear values, the rms noise power in the received signal is:

$$P_n = k_B T b \tag{4}$$

where:

P_n = noise power, W
k_B = Boltzmann constant (1.38×10^{-23} J/K)
T = noise temperature (K)
b = bandwidth (Hz).

Eq (4) can be restated in decibels:

$$P_{n;dBW} = k_{B;dB} + T_{dB} + b_{dB} \tag{5}$$

where:

$P_{n;dBW}$ = noise power, dBW
$k_{B;dB}$ = Boltzmann constant ($10\log(k_B)$)
b_{dB} = bandwidth ($10\log(b)$).

The receiver noise temperature T in kelvin is directly related to the receiver noise factor by:

$$T = 290(n_f - 1) \tag{6}$$

where:

n_f = noise factor (linear value)

Noise figure N_f is noise factor n_f expressed in decibels, so,

$$n_f = 10^{N_f/10} \tag{7}$$

The overall system noise temperature T_{sys} in kelvin is:

$$T_{sys} = T_A + T_{AP}\left(\frac{1}{\eta_1} - 1\right) + T_{LP}\left(\frac{1}{\eta_2} - 1\right) + \frac{T_R}{\eta_2} \tag{8}$$

where:

T_A = temperature received by antenna (K)
T_{AP} = antenna physical temperature (K)
T_{LP} = transmission line physical temperature (K)
T_R = receiver noise temperature (K)
η_1 = antenna efficiency (between 0 and 1)
η_2 = transmission line efficiency (between 0 and 1).

G/T Figure of Merit

G/T is a figure of merit for the receiving part of a link, *i.e.*, an earth station or the receiving part of a satellite. *G* refers to the receive antenna gain less any losses between the antenna and the first age of amplification. *T* refers to the overall system noise temperature, T_{sys}, Note that the noise bandwidth *b* is not included in the *G/T*.

From the above equations, it can be seen that,

$$P_r - P_{n;dBW} = \frac{C}{N} \qquad (9)$$
$$= \frac{G}{T} + EIRP - L_p - k_{B;dB} - b_{dB}$$

where:

C/N = carrier to noise ratio (dB)

G/T = gain to temperature ratio (dB).

By rearranging terms in **Eq (9)**, one can easily calculate the required performance of a satellite or an earth station satellite performance is limited, which makes its *EIRP* limited; this dictates how good an earth station *G/T* must be in order to achieve whatever *C/N* is needed for successful reception.

Normally the receive antenna gain of an earth station is specified along the antenna boresight. However, with a satellite this is not practical because the receiver site on the ground is often not along the satellite antenna boresight. Therefore, for satellites a two-dimensional *G/T* plot is made, thus reflecting the changing antenna gain with respect to the boresight gain.

An Illustrative Example

Consider a 2 m downlink from a satellite with an *EIRP* of 0.5 W. What sort of earth station is required for CW and SSB reception? The values used in this example are for illustration only.

Here are the known parameters:

distance between the earth station and the satellite will be from 400 km (52.04 dB) to 1000 km (60 dB).

- **frequency** downlink is 146 MHz (43.29 dB).
- **satellite *EIRP*** is 0.5 W (–3.01 dBW).
- **CW: *C/N* and required bandwidth** is 500 Hz (26.99 dB), and *C/N* is 5 dB.
- **SSB: *C/N* and required bandwidth** is 3000 Hz (34.77 dB), and *C/N* is 20 dB.

Using the above values we calculate the path loss for the two distances:

$$L_{p;400km} = 43.29 + 52.04 + 32.45$$
$$= 127.78 \text{ dB}$$
$$L_{p;1000km} = 43.29 + 60.00 + 32.45$$
$$= 135.74 \text{ dB}$$

- For *C/N* = 5 dB, 400 km, 500 Hz:

$$5 = \frac{G}{T} - 3.01 - 127.78 + 228.6 - 26.99$$
$$\frac{G}{T} = -65.82 \text{ dB}$$

- For *C/N* = 5 dB, 1000 km, 500 Hz:

$$5 = \frac{G}{T} - 3.01 - 135.74 + 228.6 - 26.99$$
$$\frac{G}{T} = -57.86 \text{ dB}$$

- For *C/N* = 5 dB, 400 km, 3000 Hz:

$$5 = \frac{G}{T} - 3.01 - 127.78 + 228.6 - 34.77$$
$$\frac{G}{T} = -43.04 \text{ dB}$$

- For *C/N* = 5 dB, 1000 km, 3000 Hz:

$$5 = \frac{G}{T} - 3.01 - 135.74 + 228.6 - 34.77$$
$$\frac{G}{T} = -35.08 \text{ dB}$$

The most stringent *G/T* is –35.08 dB. If we assume a receiver system noise temperature of 600 K, then,

$$600 \text{ K} = 27.78 \text{ dBK}$$
$$G - T = -35.08$$
$$\therefore G = -35.08 + 27.78 = -7.30 \text{ dB}$$

At first glance this would lead one to feel that an antenna gain of –7.30 dBi is adequate. There are two reasons why this will in all probability not be so. First, the *EIRP* from the satellite will not be a steady 0.5 W because the satellite antenna is not always pointing toward the earth station. This means additional *EIRP* degradation must be included. Second, another factor that degrades reception is the Doppler shift resulting from the relative velocity of the satellite with respect to the earth station. The effect of Doppler shift will depend on the receiver design.

Some Final Thoughts

The most difficult factor to calculate is noise. From attenuation, antenna side lobes, the warmth of the Earth and the sky, and so on. For most amateur satellite links, an approximation is all that is needed.

Amateur satellite data should include *EIRP* and *G/T* as a function of the compound angle from the satellite. This information will make link calculations possible. Of course, to this data must be added the degradation caused by the dynamics of the satellite itself in orbit.

Evans Wetmore, P.E., K3VFA, a ham since the 1960s,holds an Amateur Extra class. Prior to his retirement, Evans was Senior Vice-President, Advanced Engineering of the Fox Technology Group. As such he was responsible for engineering and technology for Digital Cinema for Twentieth Century Fox and for FCC and antenna work for Fox Television Stations. He began his career at PBS where he helped engineer and deploy the first nation-wide satellite television distribution system. In 1979 he migrated to Hollywood to work on Special Effects on Star Trek the Motion Picture, Brainstorm, and Bladerunner. He is a Fellow of SMPTE and an Associate Member of the ASC. He authored the Optical Formula section of the ASC Handbook. Evans holds multiple patents and is a registered professional engineer in North Carolina and California. He got his degree in Electrical Engineering from Duke University.

John O. Stanley, K4ERO
524 White Pine Ln., Rising Fawn, GA 30738; **jrnstanley@gmail.com**

Verification of the Short/ Open Method of Measuring Small Network Losses

Practical and simulated examples of its use, and of the errors are discussed, along with their source and a correction method.

I have been researching a method to measure loss in a network, especially useful for antenna tuners, along with presenting some examples of where and why the method sometimes gives erroneous results. The method excels when losses are low, which is where other methods are error prone. This document contains many examples of the use of the method along with both practical and simulated examples of its use. Errors are discussed, their source along with a correction method.

The method is very similar to the method long used to measure coaxial cable loss, and which has recently been refined by showing the need to use both a short and an open on the far end, and to take half the average (in dB) of the two return loss values. Failure to do so can lead to large errors in certain cases, for example when the line is electrically short and has high loss, combined with a complex Z_0, which is not uncommon. See references **[1]**, **[2]**, **[3]**, **[4]**, and **[5]** for recent works on this topic.

The most lossy networks normally used in electronics are attenuators. Some attention will be given to how the method can be used to measure such devices and what it means if the method gives strange results. At the other extreme are matching networks where it is normally desired to have as little loss as possible. In between are filters where some considerable loss might be accepted in the interest of passing some frequencies preferentially and rejecting others.

My analysis will use SPICE (QUCS) simulations to get a feel for accuracy of the method, and the cases where it can give misleading results if the limitations are not properly understood. This will be supplemented with real world tests to confirm that the SPICE simulations are realistic. The QUCS screen will be shown in the terminated condition. The S11o/s values are taken by adding a short or open to the circuit and running the simulation, then recording the values. These screens are not shown in the interest of space.

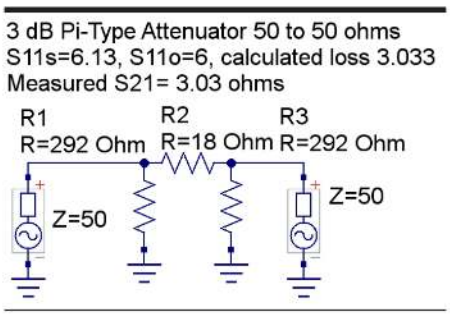

Figure 1 — 3 dB 50 Ω attenuator.

Attenuator tests

See the **Sidebars – Definition of Terms**, and **Test Method for Networks**. A 3 dB attenuator (**Figure 1**) was analyzed and the simulation showed that S11s and S11o should both be about 6 dB. (S11o+S11s)/4 should show 3 dB. This is confirmed to be the

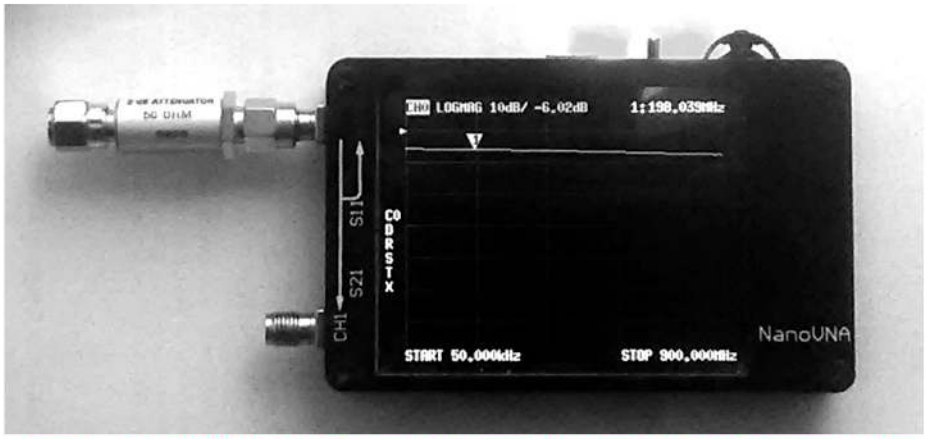

Figure 2 — S11s (CH1 LOGMAG) as read on a nanoVNA. There is a short connected to the output of the attenuator.

same as the S21 (through path) calculation to within a small error. This error can be rounding errors or due to the resistor values not being exactly the calculated values.

The nanoVNA (**Figure 2**) indicated values near 6 dB (varying somewhat with frequency) for a calculated loss of 3 dB ±0.05 dB. This test might seem unnecessary, but it confirms that the pad is undamaged and, if its label is lost, could reveal the loss value. One can also see how perfect the pad is vs. frequency. Of course, the nanoVNA could also do a check using the S21 (through) connection.

A useful attenuator is the "minimum loss" 50 to 75 Ω pad (**Figure 3**). This matches 50 to 75 Ω with a good match on each end. The design can be made with more loss than the minimum, but not less and still have the ends matched. This shows that the method works even when input *Z* and output *Z* are different.

This 20 dB pad will match 50 to 500 Ω (**Figure 4**). The calculated loss from the S11s and S11o is exactly the same as the S21 value. The perfection of the method is ensured by the very precise values used for the resistors. In the real world such precision would not be possible but close enough to make the loss calculation method useful. What if both ends are not matched to the network? Consider a "network" consisting of a single 40 Ω resistor between a 50 Ω source and a 10 Ω load (**Figure 5**). The input (S11) will be matched, but on the load side there will be a very bad mismatch. With a short on the output the input will still nearly match (S11s = −19.1 dB) but with the open, it will not (S11o = 0 dB). The calculated loss will be 4.85 dB, but S21 shows 6.99 dB. Thus, the error will be 2.14 dB, clearly a serious error. Changing the "network" to a 20 Ω resistor, feeding a 30 Ω load reduces the error to 0.38 dB and changing it to a 10 Ω resistor feeding a 40 Ω load reduces the error of the method to 0.09 dB. Further tests showed that the error could be explained fully as additional loss due to the mismatch at the output, S22. That the error is due to S22 mismatch can be confirmed by comparing the loss error to the mismatch loss in **Figure 6A** and its expanded version **Figure 6B**. For example, with the 40 Ω resistor, SWR is 9:1 and the unaccounted for loss is 2.2 dB, as nearly as can be read, compared to the calculated 2.14 dB. Likewise with the 10 Ω resistor, the output side SWR of 1.5 leads to 0.1 dB error (0.09 calculated with the S11o/s method). **Figure 7** relates SWR to return loss in dB.

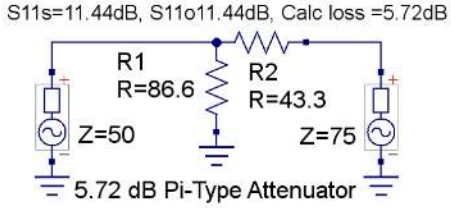

Figure 3 — 50 to 75 Ω "minimum loss" attenuator, with 5.72 dB loss.

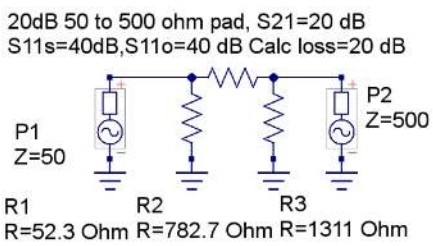

Figure 4 — 50 to 500 Ω attenuator with 20 dB loss.

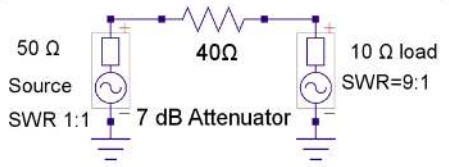

Figure 5 — Badly designed attenuator pad. The input (S11) will be matched, but on the load side there will be a 9:1 SWR. The S11o/s method is not accurate for this network.

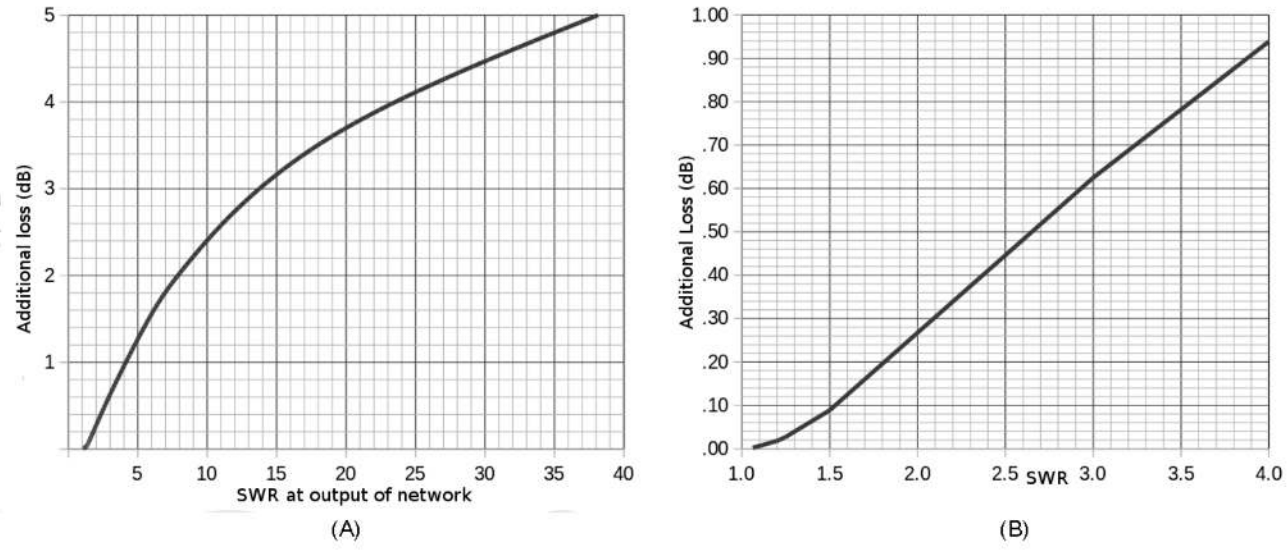

Figure 6 — Chart (A) shows the additional loss caused by a mismatch at the output of a network due to the mismatch. An expanded version (B) allows more precision for low SWR values.

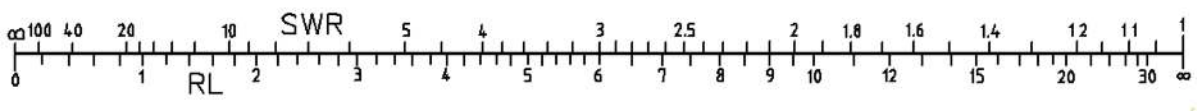

Figure 7 — Handy scale for converting between return loss (RL) in dB and SWR.

The method applied to lossless networks

Here is an **L** network (**Figure 8A**) to match between 50 and 200 Ω. There are no losses in the components, so there will be no "through loss" (S21) provided that the components are properly tuned. This approximates an antenna tuner that is properly adjusted. As one would guess, S11o and S11s are both 0 dB since there is simply no place for any loss to occur. With the load removed, no resistance is found anywhere in the network, so conservation of energy alone says that there can be no loss anywhere *in the network* — we did say it was a lossless network. However, if the network is improperly tuned as in **Figure 8B**, there will be a mismatch loss on *both* ends. This will not be accounted for by the S11o/s method. The mismatch at S11 and S22 will both be the same, which is a characteristic of lossless networks. A return loss of 12.7 dB equates to an SWR of 1.6 and a matching loss of 0.12 dB at each end. This gives us a total matching loss of 0.24, close to the 0.239 total loss calculated by the S21 method.

This example tells us something rather obvious. One should tune any tunable network to a match on at least one end, normally the end with the transmitter. If the losses are very small, this will tune both ends and there is no chance of a mismatch causing additional loss. As the losses increase, tuning one end may or may not tune both ends as we will see in the next examples. But even with a lossy network it is possible to have both ends matched. In that case the S11o/s method works perfectly.

A tuner with loss that works very well with the S11o/s method

This tuner (**Figure 9**) is very well matched on both ends, but has some loss in both the inductor and the capacitors. The S11o/s method works very well. However, to get this result we had to assume the same unloaded Q for each component, which is not realistic in that inductors typically have a lower unloaded Q than capacitors.

Figure 10 shows an example of a **T** network tuner that when matched on the input side will have 1.09 SWR on the output side. Nevertheless, the S11o/s method gives

Definition of Terms

S11o – is the magnitude in dB of the return loss with the output open.

Labeled CH0 LOG MAG on nanoVNA in dB.

S11s – is the magnitude in dB of the return loss with the output shorted.

Labeled CH0 LOG MAG on nanoVNA in dB.

S21 – is the voltage ratio between output and input of the device under test. When followed by a dB, it is the same ratio in dB. S12=S21 for passive networks.

Labeled CH1 LOG MAG on nanoVNA in dB.

S11 – is the complex voltage ratio of the wave reflected from the input of a network.

S22 – is the complex voltage ratio of the wave reflected from the output of a network.

S11 and S22 are best observed on a Smith Chart display.

frequency	dBS11	dBS21	dBS22
1e07	-69.1	0	-69.1

S11s=0dB, S11o=0dB, Calc loss =0dB

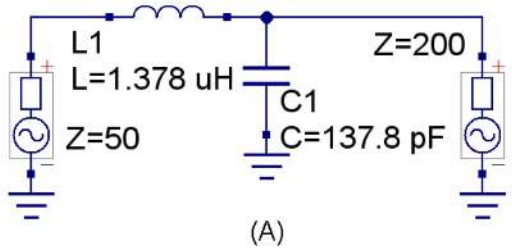

(A)

frequency	dBS11	dBS21	dBS22
1e07	-12.72	-0.239	-12.7

S11s=0dB, S11o=0dB, Calc loss =0dB

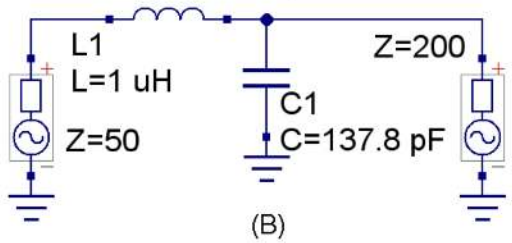

(B)

Figure 8 — L networks (A) and (B) used to show that mismatched loads cause S21 loss.

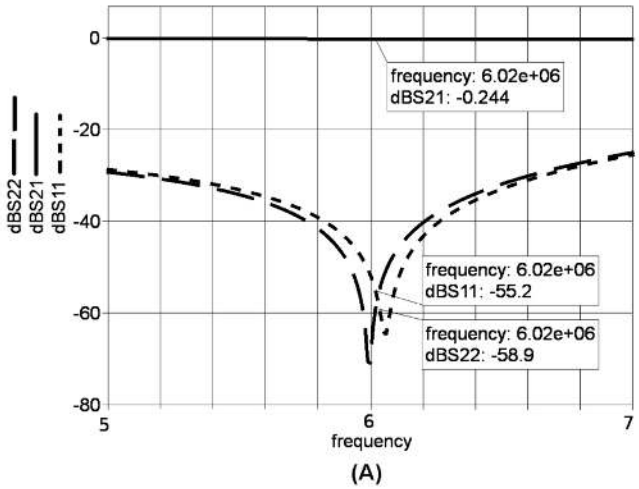

(A)

Pi tuner with nearly the same QU for all components
S11s=.512, S11o=.463, cal attn=.24375 S21=.244

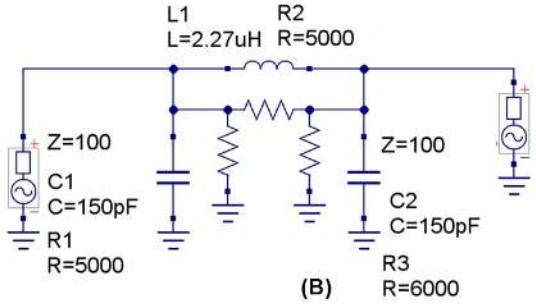

(B)

Figure 9 — The response (A) of a lossy network (B) that is matched on both ends.

the correct answer to three decimal places. This is because a 1.09 SWR, as shown in **Figure 6B**, introduces no significant amount of mismatch loss in addition to the calculated value. **Figure 18B** will confirm this.

In contrast to the above example, **Figure 11** is a case where the S11o/s method gives significant error. Matching into a low resistance load, which commercial tuners often do poorly, we see that the calculated value is 1.36 dB, whereas the true loss is 1.67. This extra 0.31 loss can be explained by noting that the mismatch on the output side is 9.32 dB return loss, or 2.05 SWR, which from **Figure 6** and **Figure 7** shows an extra mismatch loss of 0.26 dB. In this example, the method is not very accurate, but it does serve to warn that the tuner loss is high.

dBS11	SWRin	dBS22	SWRout	dBS21
-52.2	1	-27.5	1.09	-0.193

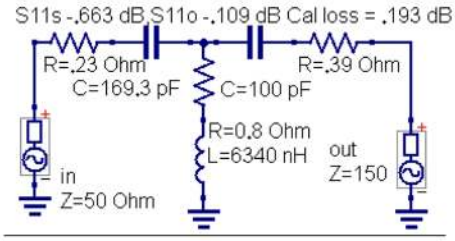

Figure 10 — Typical T network tuner.

frequency	dBS11	dBS21	dBS22
1e07	-29.06	-1.67	-9.32

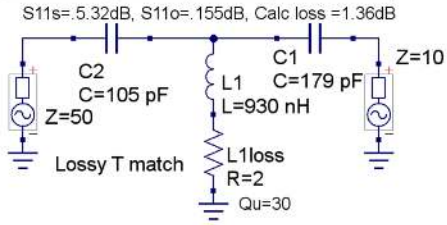

Figure 11 — T match tuner feeding a low *Z* load.

frequency	dBS11	dBS21	dBS22
1e07	-34.45	-0.756	-15.1

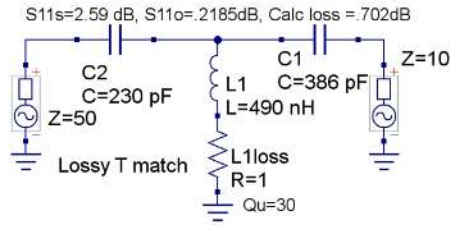

Figure 12 — T match better adjusted for feeding the low *Z* load.

If we use less *L* and more *C* in tuning to this 10 Ω load (**Figure 12**) we find that the calculated loss is halved, and the error is reduced from 0.31 dB to only 0.054 dB, that is, it is reduced by 80%. This further illustrates that the S11o/s method is very accurate for low loss values, but has more error when the losses are higher. We also notice that as losses go higher, the match on the output side is worse when we match the input side. This is what causes the error to increase.

How unbalanced loss in tuned networks causes a mismatch on the output end

What causes the mismatch on the output side as we tune for match on the input side? It seems it is not just loss in the components, but unmatched loss between the series and shunt elements that is the problem. If it were only loss that causes the problems, the attenuator pads would not work at all with this method, since they have very high loss. But we know that an attenuator that is missing the shunt resistors fails badly in this measurement method. Antenna tuners can make the *Z* looking into the network be 50 Ω even for loads that depart considerably from 50 + *j*0 Ω. However, it is not always realized that the output side of the tuner does not necessarily provide a perfect conjugate match to the *Z* looking into the transmitter end of the coax. This problem is caused by "unbalanced" losses in the tuner.

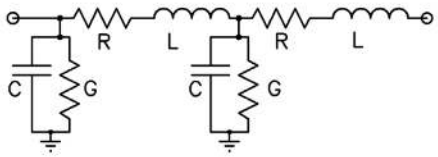

Figure 13 — Model of a transmission line with loss. The *R* and *G* represent the resistance in the wire and the leakage in the insulation.

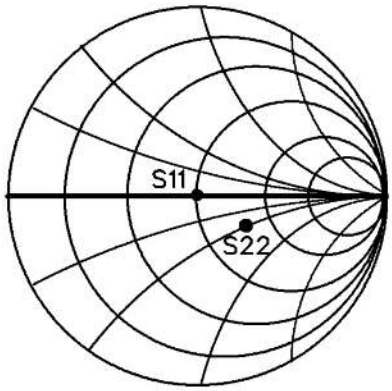

Figure 14 — Effect of matching the input of a circuit with unbalanced losses between the series and parallel elements.

It has been known for many years that transmission lines, which are a type of network, may not have the same losses in the conductor as it has in the insulating medium. An ideal transmission line (**Figure 13**), which is modeled as an infinite number of infinitesimal **pi** or **T** networks will have an inductance *L* per unit length, and capacitance *C* per unit length and with no losses, the Z_0 will be:

$$Z_0 = \sqrt{\frac{L}{C}}$$. However, including the losses,

$$Z_0 = \sqrt{\frac{R + j\omega L}{G + j\omega C}}$$.

If the amount of loss in the inductors (conductors) is equal per unit length to the loss in the capacitors (insulators) the line will have a purely resistive Z_0, typically 50 Ω for coaxial lines and 600 Ω for balanced (telephone) lines. When the two types of loss are unequal, strange things happen. The Z_0 of the line will be complex. On telephone lines this causes problems that were solved by inserting additional inductance every mile or so (the familiar 88 mH chokes) so that the ratio of *L/C* and *R/G* will be the same, see: **https://www.prc68.com/I/Inductors.shtml**.

When loss is added to a circuit, the match points on the input and output move away from a match but in opposite directions. If we adjust for a match at the input S11, as is normally done, the output mismatch S22

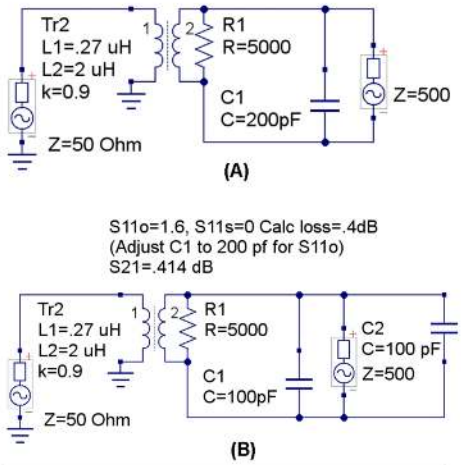

Figure 15 — Link coupled tuner (A) for balanced loads. In (B) part of C1 is put on the output to represent a reactive load.

will be pushed further away from a match when the losses in the tuner are unbalanced between the series and shunt elements. This is illustrated in the Smith Chart of **Figure 14**.

With coax, we simply live with the issues as they are usually quite small. To see how small, put a 50 Ω load on a coax using the TLW program and see what the Z_{in} is at the input end of the coax. It will be close to 50 Ω but not exactly that due to the complex Z_0 of the coax.

What about reactive loads?

All of the simulations done to this point have had resistive loads. In the real world, loads such as antennas are often reactive. Previous testing methods for tuner loss have typically allowed only resistive loads to be evaluated. In the example here (**Figures 15A** and **15B**), the 200 pF capacitor, *C*1, was divided between *C*1 and *C*2 and in parallel with the 500 Ω resistive part. Each of these was set to 100 pF. This represented a load with a negative parallel reactance. When the short was applied, the S11s value was the same with either tuner. However, when the open was applied in the **Figure 15B** circuit, thereby removing both the 500 Ω load and the 200 pF part of the load, the network was detuned and the S11o value was not the same as in the above example. Thus, the total loss calculation was incorrect. However, by adjusting *C*1 to 200 pF instead of the 100 pF that remained, the method worked well. This illustrates that when a reactive load is involved, adding the short or open can pull the tuner out of resonance. Since loss is maximum at resonance as circulating currents increase, it was evident that when loads are reactive, one must retune to resonance when doing the S11o or S22s loss measurements. This adjustment should be made only to the component on the output side of the tuner when possible. This could be either a series or parallel element, and either an *L* or a *C* depending on the tuner configuration.

Figure 16 is a **T** match feeding a reactive load. It is adjusted to resonance. The capacitor labeled *jXc* is the reactive part of the load while the *R* is the real part. This load reactance affects the resonant frequency. When the open is applied to the network, *C*2 is effectively removed from the circuit as one end of it is floating. When the short is applied, *C*2 is active, but the capacity in the load is not. *C*2 must be readjusted to resonance, which puts the effect of the reactive part of the load back into the circuit. If the short could be connected to the junction of the real and reactive part of the load, the resonance would not shift, but that is not possible.

In some cases, it may not be possible to re-resonate the network. This could be due to limitations in the adjustment values of the output component or inability to adjust that component manually in the case of an autotuner. If resonance cannot be restored when making the measurements, the calculated loss will be *less* than the true value. This is in contrast with the errors that result from output mismatch, which always add to the measured value. Apart from adding an external component to extend the match range of the network, I have no other suggestion as to how resonance could be restored when either of these problems exist. We can consider this condition to represent a case for which this method is not suitable. It will only exist with highly reactive loads, probably those barely within the tuning range of the network itself.

To see if this method is limited to **T** networks, a simulation was made of a link coupled balanced tuner, **Figure 17**, which shows a plot of S11 with the load disconnected (S11o). The resonance was restored by tuning *C*5 so that the S11o was maximum at the test frequency. Since resonance increases the current in the network, loss is maximum at that frequency. The Smith Chart display provides a quick

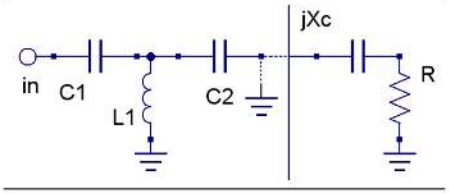

Figure 16 — T match with a reactive load.

Test Method for Networks

Install a load (resistor or antenna) on the output of the antenna tuner. Tune for best match. Remove the load and put a short on the output, record S11s. Replace the short with an open and record S11o. Add S11o to S11s and divide by 4. This gives the loss of the network.

If the load is reactive, as is typical with antennas, you must readjust to resonance (where the S11 value is worst) before taking the S11 values, using only the tuner adjustment that is at the output of the network.

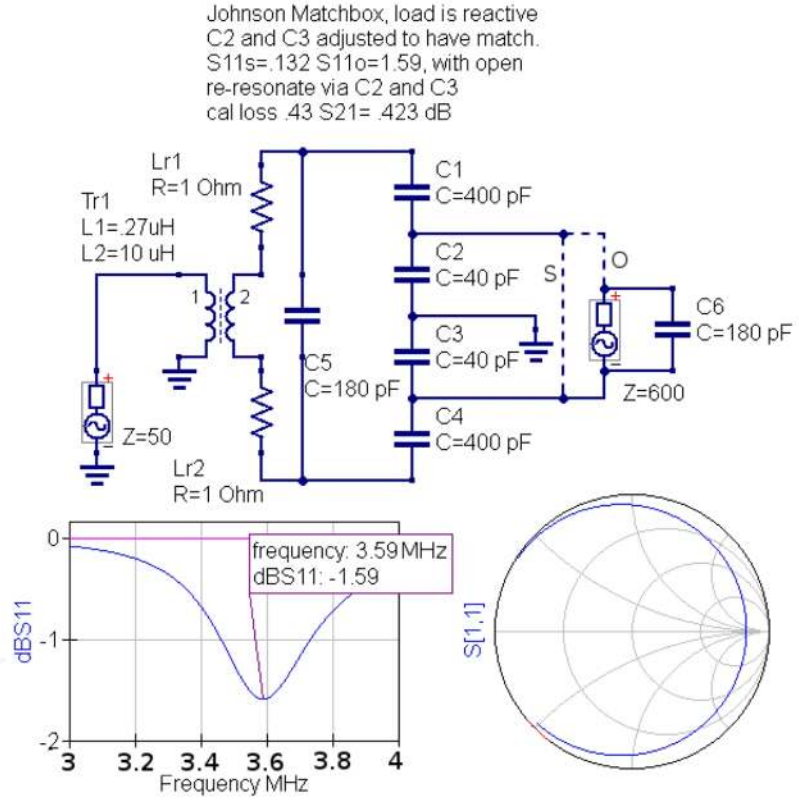

Figure 17 — Analysis of the Johnson Match Box tuner.

look at losses. With either the short or open, one wants the curve to be as far from the center as possible indicating a load that is mainly reactive. One can also see that at resonance the loss is greatest. This is the point where the curve crosses the jX=0 line.

The inductor was modeled with series resistors that represent its finite unloaded Q value. The loss was calculated by S21 to be 0.423 dB. The S11o was then seen to be 1.59 dB and the S11s was 0.132 dB. This gave 0.43 dB total loss. The input was matched at the expense of the output match. Since the output mismatch was small, the error was not significant (0.007 dB). When the open was present, the resonant frequency shifted above 4 MHz. Adjusting *C*2 and *C*3 to 400 pF each brought it back to resonance at 3.59 MHz. But it is not possible to adjust *C*2 and *C*3 apart from *C*1 and *C*2 in the real world Johnson Matchbox (**Table 1**) because they are ganged with *C*1 and *C*3, so resonance was also tried instead by adjusting *C*5. This gave essentially the same result. Real world tests with an actual Johnson Matchbox showed similar behavior. The main "Tuning" dial (*C*5) was used for resonance, not the "Matching" dial (*C*1 – *C*4).

Error correction for high loss values

Even though the S11o/s method does not account for additional loss due to a mismatch at the output, there is a way to estimate those losses fairly accurately. The charts of **Figure 18** were devised to allow one to account for the losses due to S22, even if it is difficult or impossible to measure them as will normally be the case with all but 50 Ω loads.

WARNING: Cases where the tuner was either not properly tuned, or the tuner not re-resonated when testing a reactive load, are not correctable as they represent blunders in applying the method, not errors in the method itself.

A plot of S11o/s measured values vs. S21 values shows that the errors are small when the loss is small. They are also small when the shunt and series arms of the network are equally lossy, which makes the S11o and S11s values nearly equal. When losses are more than 1 dB, the mismatch at the output can be large when tuning for match at the input. If we know the mismatch at the output, we can calculate the mismatch loss using the SWR vs. mismatch loss charts of **Figure 6**. This works fine with simulations, but with real world networks may be difficult or impossible. But we can estimate the expected error by taking the absolute value of the ratio of S11o and S11s readings. If the S11o and S11s value ratio is close to 1, the error is negligible. If it is about a three to one ratio, the error will be near the curve labeled 3 in **Figure 18A**. If the ratio is over 40 to one, the error will be near the infinity curve. The additional loss due to mismatch then can be added to the S11o/s calculated loss for a corrected value. An example from **Figure 18** would be a tuner that measures 3 dB with the S11o/s method. Its true loss would be between 3 and 4 dB depending on the S22 mismatch loss. Which of these is closest to the correct value can be estimated from the absolute value of the S11o to S11s ratio. If that ratio is near 3:1, the curve labeled 3 would give the excess loss estimate, so we would assume a true loss of 3.26 dB. If the ratio is high, true loss could be 4 dB.

These curves were derived from the results of many simulations. I believe they are accurate to within about 0.05 dB for high losses, and 0.02 for low losses. It is likely that formulas could be developed to provide a more exact correction factor, but I have not attempted that. There seems to be a definite relationship between S11o, S11s, S22 and the error value. When errors are present, the actual loss is more than the measured loss. Even without correction, this method can serve to indicate that the load being matched is not being fed power in an efficient way. Either readjustment or redesign of the network may be called for.

Table 1 – Tests on the K4ERO Johnson Matchbox.

Freq., MHz	*Load, Ω*	*S11o, dB*	*S11s, dB*	*Loss, dB*	*Efficiency*
3.7	68	1.4	1.0	0.60	87.1%
3.7	390	0.96	0.91	0.47	89.9%
3.7	1 k	0.73	0.83	0.39	91.4%

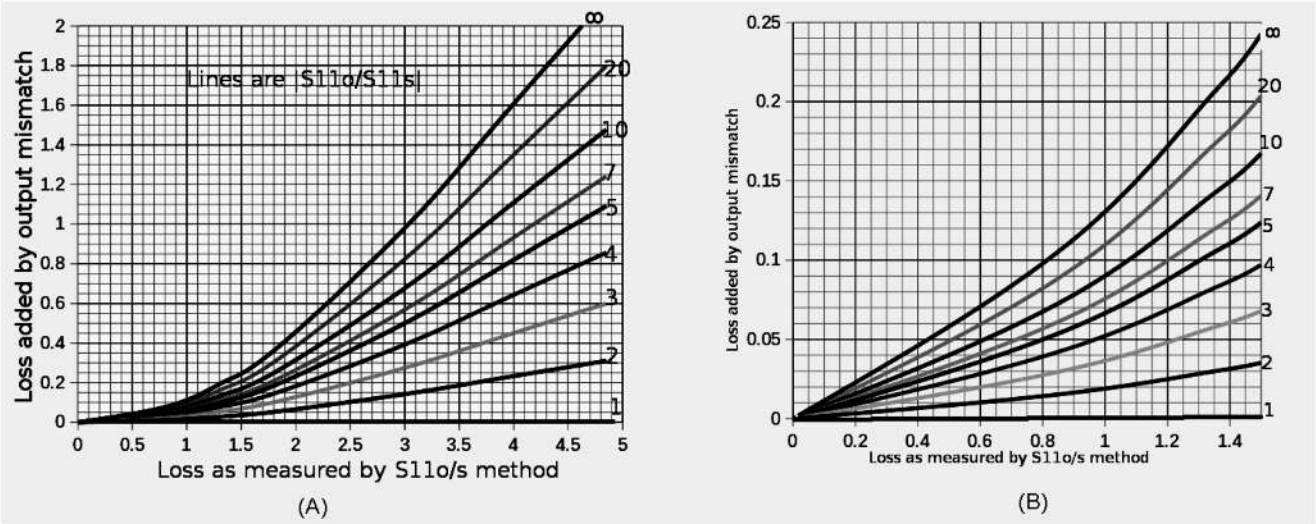

Figure 18 — Correction factor (A) for networks where the S11o and S11s values differ. Use the curve corresponding to the absolute value of the S11o and S11s ratio. (B) shows an expanded scale for low values of calculated loss.

John Stanley, K4ERO has contributed many articles to QST, QEX and other ARRL publications. He co-authored two chapters in the NAB Engineering Handbook. John received the ham call KN4ERO 67 years ago and has been active ever since. John, aided by his wife of 53 years Ruth, WB4LUA, spent most of his working life doing training, consulting and other engineering work at Christian shortwave stations in many countries . They now live on Lookout Mountain in Northwest Georgia.

Notes

[1] J. Stanley, K4ERO, "Precautions When Using the Return Loss Method of Measuring Coax Loss," *QEX,* Jan./Feb. 2022, pp. 21-22.

[2] F. Witt, AI1H, "Improved Accuracy in Antenna Tuner Evaluation (Technical Correspondence)," *QST,* Oct. 2003, pp. 73-74.

[3] P. Salas, "Antenna Tuner Loss Measurements," *QEX,* Mar./Apr. 2021, pp. 3-9.

[4] J. Stanley, K4ERO, "Calculating Transmission Line Loss with SWR Readings (Technical Correspondence)," *QST*, Oct. 2021, p. 55.

[5] F. Witt, AI1H, "Measuring Cable Loss," *QEX*, May/Jun. 2005, pp. 44-47.

Upcoming Conferences

ARRL/TAPR Digital Communications Conference

September 16 – 18, 2022
Charlotte, North Carolina
www.tarp.org

The 41st Annual ARRL/TAPR Digital Communications Conference (DCC) is scheduled for September 16 – 18, 2022, in Charlotte, North Carolina.

Make your reservations now for three days of learning and enjoyment at the Hilton Charlotte Airport Hotel. The DCC schedule includes technical and introductory forums, demonstrations, a Saturday evening banquet, and an in-depth Sunday seminar. The DCC is for everyone with an interest in digital communications — beginner to expert. See website for details. Note that all plans are subject to change due to Coronavirus.

Conference papers will be distributed as PDFs to DCC attendees. Printed copies of the papers will be available for sale at Lulu **(www.lulu.com)**.

6th Annual 2022 Pacific Northwest VHF Society Conference

Oct 7 – 8, 2022
Salem, Oregon
www.pnwvhfs.org

The 6th Annual 2022 Pacific Northwest VHF Society Conference will be held Friday – Saturday, October 7 – 8 at the Holiday Inn Hotel, 3301 Market St. NE, Salem, OR 97301. Conference registration is $65 before October 1, or $75 thereafter and at the door. See website for more information.

40th Annual AMSAT Space Symposium

October 21 – 22, 2022
Bloomington, Minnesota
www.amsat.org

The 40th Annual AMSAT Space Symposium will be held October 21 – 22, 2022, at the Crowne Plaza Suites hotel in Bloomington, Minnesota.

Call for papers: Proposals for symposium papers and presentations are invited on any topic of interest to the amateur satellite community. We request a tentative title of your presentation as soon as possible, with final copy submitted by October 14 for inclusion in the symposium proceedings. Abstracts and papers should be sent to Dan Schultz, N8FGV, at n8fgv@amsat.org.

H. Lawrence Serra, N6NC
1135 Torrey Pines Rd. Apt. 2C, La Jolla, CA 92037; **hlserra@gmail.com**

Why Summer 40 m Propagation Is So Good Between Japan and the US Pacific Coast

Summary of an investigation into the physical causes of enhanced 7 MHz summer trans North Pacific propagation.

For seven months I checked every source of data available, consulted RF, oceanographic and meteorological experts, researched and dismissed competing meteorological and RF theories, and concluded that enhanced 40 m CW summertime trans North Pacific propagation is the result of smooth sea RF reflection points under huge summertime Pacific high pressure areas

CW Skimmer as a Propagation Tool

In 2008 Alex Shovkoplyas, VE3NEA, invented the *CW Skimmer* software. I saw the opportunity for a local skimmer to be an effective contest and propagation tool, so with an SDR I was set to monitor and log nightly 7 MHz CW signals received at my San Diego, California location. From San Diego, 7 MHz had always provided excellent nighttime propagation to DXpeditions on the Pacific Islands, so I was interested in HF propagation between San Diego and Japan. At the same time I designed and installed at my location, 700 yards from the Pacific Ocean, a 40 m 2-element parasitic vertical array aimed directly at Japan and the Asian coast, bore-sighted at 315°, and a switching network to feed the antenna to the SDR and *CW Skimmer* from 9 pm to 9 am local time to monitor nighttime CW signals from the Asian coast.

This was useful for a year, showing me occasional JA call signs received overnight across the Pacific. Then on a Saturday morning, July 24, 2010, I looked at the call signs collected overnight by *CW Skimmer* and discovered 141 JA call signs recorded between about 07:00Z and 15:00Z (12 am – 8 am PDT). 80% of them were in the 3 hours between 08:00Z – 11:00Z (1 am – 4 am PDT). I remember being astonished, because the *CW Skimmer* had never recorded more than a couple of JA 7 MHz call signs overnight, and I noted the event in memory.

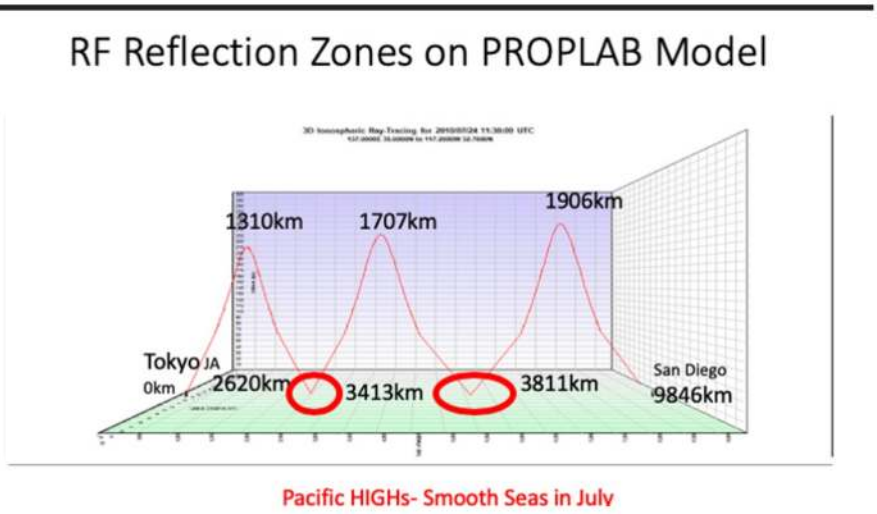

Figure 1 — *PROPLAB* 3-hop Tokyo – San Diego model for July 24,2010, with superimposed data.

Investigation

JE1CKA: I emailed contester Tack Kumagai, JE1CKA, to ask him why I received all those calls at one time. He said it was the date of the annual Japan summer domestic CW contests, but what astonished him was that 85% of the call signs were from 5 watt JA CW stations!

USN Radio Ops: I tried to locate retired USN radio operators who had sailed the Pacific in WWII to learn their anecdotal understandings of summertime 7 MHz propagation, but sadly most had passed.

Reverse Beacon Network (RBN): I checked the RBN data for July 24, 2010. My N6NC 141 RBN JA spots represented 14% of all RBN 7 MHz JA spots from all around

the world on that date, an unusually large percentage. The average signal-to-noise ratio of those 141 reported JA call signs was 10.9 dB.

WSPR, PSK, GPS TEC Data: I examined data from *WSPR* and *PSK Reporters*, GPS satellite Total Electron Content (TEC) data, gray line enhancement and PMSEs. Specific data was either inapposite, or did not exist for July 2010.

VOACAP Propagation Data: *VOACAP* propagation data is available online to hams with interfaces such as Jari Perkiömäki's, OH6BG, app **voacap.com/hf/** and Alex Shovkoplyas', VE3NEA, *HamCAP* program **dxatlas.com/hamcap/**.

I studied *VOACAP* data. I used both ham interface programs and ran the *VOACAP* profile for 7 MHz (40 m) on July 24, 2010. To my surprise, the data showed the 7 MHz month of July propagation circuit reliability between Tokyo and San Diego to be between 90% and 100% for 5 – 6 hours/day based on years of *VOACAP* data.

K9LA *PROPLAB* Model

I corresponded with propagation guru Carl Luetzelschwab, K9LA, an RF engineer with industry experience and many amateur propagation experiments, to see if he had any idea what caused the trans Pacific propagation anomalies. Carl generally relies on the data from ionosondes located at the middle of propagation paths to determine what and how many ionospheric hops have occurred to complete the HF circuit, and he modeled for me in *PROPLAB* a 3-hop potential 7 MHz path (**Figure 1**).

So a *PROPLAB*-predicted 3-hop, 2 sea surface reflection path actually existed, and my 10.9 dB SNR average for the 141 JA call signs on July 24 was not entirely anomalous, but an unusually good time of the year for 7 MHz trans Pacific propagation.

Path-End Ionosondes

Unfortunately, there are no ionosondes located along the great circle path between San Diego and Tokyo across the North Pacific, depriving us of vertical ionospheric data along the path. I discovered that there were ionosondes located close to each end of the propagation path, so I checked the archives of the Wakkanai-Hokkaido, Japan and the Point Arguello/Vandenberg AFB (Los Angeles) ionosondes for data at each path end. I noted that virtually the entire North Pacific along the path was in the dark on that date; darkness generally reduces the MUF along the path.

The Wakkanai and Point Arguello ionosondes both reported vertical overhead MUFs of around 3.3 MHz, too low for 7 MHz propagation. However, I noticed at the bottom of the ionosonde report charts for July 24, 2010 that a table showed slant range MUFs based on low angle waves traveling long distances through a cumulatively denser ionospheric electron layer determined by the length of the hop. This scale showed at ~1550 km seaward from each coastal ionosonde — the midpoint of a ~3100 km hop — the MUF was as high as 12.4 MHz, good for 7 MHz propagation. The total electron density at 1550 km seaward from each path end caused a refraction in the ionosphere of the low angle 7 MHz HF wave back down toward the ocean's surface at a point 3100 km further seaward from both ionosondes.

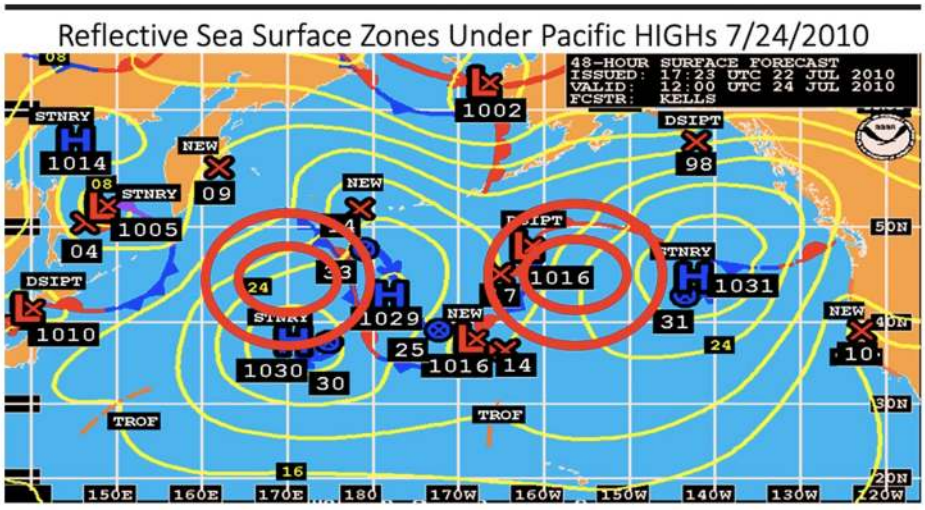

Figure 2 — The concentric shapes indicate RF graze zone / reflective sea surfaces on north Pacific synoptic weather chart.

RF waves refract in the ionosphere, and reflect from the ocean's surface. Refraction produces the offset image you see when you place a ruler in a glass of water. These slant range MUFs meant that with a similar middle hop, the 3-hop path completed and would connect the two hops emanating seaward from each coast.

PROPLAB Ray Trace Models

I returned to Carl's 7 MHz 3-hop *PROPLAB* model ray paths across the north Pacific on July 24, 2010. The three-hop model showed a 90%-100% reliable 7 MHz *VOACAP* circuit in July between Japan and the US Pacific coast based on years of *VOACAP* data. But due to ionospheric/atmospheric absorption, and likely rough sea reflection losses, I initially thought the 3-hop path across the Pacific was unlikely. That is, until I went back and reviewed the detail of the *VOACAP* data which showed the takeoff angle (TOA) of the strongest signals for the date, time, and ionospheric condition. The *VOACAP* TOA graphs showed maximum transmitted signal strength at 8° and 10° elevation TOAs. The *EZNEC* model of my two element, 40-meter parasitic array aimed at Japan showed a maximum signal elevation angle of 10° and +8 dBi gain.

While there is no direct correlation between TOAs and AOAs (angles of arrival), in discussions with Carl, K9LA, we concluded that the low angle, strongest TOAs from Asia usually arrive strongest here in San Diego at close to the same low AOAs — within ±0° to 2°. In this case both maximum signal TOAs in Japan (8° and 10°) and the 10° maximum signal elevation angle of my vertical array in San Diego were the same. I concluded it is unlikely for a 10° TOA to be received at a substantially different AOA, barring the infrequent occurrence of certain atmospheric and meteorological conditions, which did not exist on July 24, 2010.

Interferometer

To verify the assumption about TOAs and AOAs, I created a make-do interferometer with which to gauge the AOA of HF RF signals at my QTH. Over several months the interferometer was tested on shortwave signals from around the world. Remarkably, almost uniformly, the reported AOAs of these HF signals were within 0° to 2° of the reported *VOACAP* TOAs at the transmitter locations, confirming the 10° TOA and AOA of the JA RBN spots.

Smooth Sea, Calm Water RF Reflections

In a 2017 *CQ Magazine* article **[1]**, David Day, N2DAY, suggested that data analysis showed a likelihood of stronger US ham 160 m CW spots recorded in Europe when the Atlantic Ocean wave heights were less than 3 m (10 ft) high. Earlier US Navy and other research papers generally did not address smooth sea propagation under summer North Pacific Ocean high pressure centers, but the Day article tended to confirm my guess about smooth sea states enhancing signal strengths.

I found recent papers **[2]**, **[3]** dealing with the issue of the RF reflectivity from smooth or rough ocean surfaces. Li **[2]** contended that for a smooth ocean surface, RF waves refracted down from the ionosphere were reflected as specular waves off the ocean surface — that is, near perfect reflection, angle of incidence equals angle of reflection — and incur virtually no loss in reflection off the smooth ocean surface. Wang **[3]** shows the same result — near lossless HF wave reflections off a smooth sea surface, and zero loss in the ionosphere.

Specifically, Figure 3 in **[2]** gives the reflection coefficient for the calm sea vs. frequency. At 7 MHz, it's about 0.975. Thus, 20log(0.975) = –0.2 dB. For the rough sea in Figure 4 of **[2]** the reflection coefficient at 7 MHz is about 0.5, so 20log(0.5) = –6 dB. That shows 5.8 dB more loss per reflection from a rough sea compared to a smooth sea **[4]**. Smooth sea could make the difference for the propagation of weak JA CW signals on July 24, 2010.

All this suggested Carl's *PROPLAB* three-hop 7 MHz path for July 24, 2010 was increasingly likely. But of course, this assumed smooth sea at the ocean reflection points of the HF waves. How could one ever assume that anything as big as the largest ocean in the world would have smooth sea areas?

Mariners' Observations of Dead Calm Under Summer North Pacific Highs

I discussed my findings with a 40-year sea-going captain ham friend, and we both concluded that a physical cause for the propagation most likely was the summer North Pacific highs. Any sailor who has participated in the summertime TRANSPAC Race from Los Angeles to Hawaii knows that the easterly-most summertime North Pacific high is the bane of racing sailors, because the high(s) — oval blobs sometimes stretching 800 miles wide on an E-W axis — must be skirted in order to avoid sailing through their middles where the water is often dead calm, mirror-flat with zero wind. Quoting from **[5]**:

"Within this high pressure area, winds typically are light or nonexistent. In June or July, for example, winds outside the high might range from 10 to 25 knots, whereas winds inside would range from 0 to 10 knots, the lightest wind strengths being positioned near the center. Indeed, when our sailboat has been positioned near the center of the high, we've seen a mirror-smooth, seemingly painted ocean. Sometimes the only thing left to do is to swim in 18,000 feet of ripple-less, crystalline water."

Sailing through these annually occurring highs is likely why Ferdinand Magellan named it the "Pacific" Ocean. See, generally **[6]** about summertime North Pacific wind conditions.

I compared the highs to Carl's *PROPLAB* three-hop, 7 MHz trans-Pacific path and found them to closely coincide on a slightly south-skewed path (**Figure 2**).

HF great circle propagation paths can often be skewed ±50°off the center of the path **[7]**. From **[8]**, "Evidently, with the path under midnight conditions, ionization has diminished to where the great circle signal is no longer supported, but a signal from a scatter region to the west is capable of being propagated."

Multiple Diffuse Scattering

Even more likely, the low sea state on July 24, 2010 could likely have enhanced the specular RF wave arriving at San Diego by means of multiple diffuse scattering, whereby the received signal is the sum of all possible paths — not only the specular wave.

From **[9]**, "Multiple diffuse scattering can occur for every launched wave that reflects from the ionosphere; the received signal is the sum of all possible paths, such as the one shown in orange, not just the specular reflected ray shown in red." See **Figure 3**.

Path Wave Heights

The National Weather Service (NWS) archive charts showed model-predicted maximum wave heights of 1.5 m (5 ft) during that time, see **Figure 4**. But the

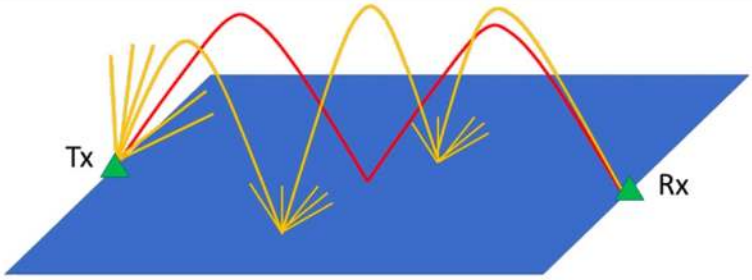

Figure 3 — Illustration of multiple diffuse scattered waves on a 2-hop model.

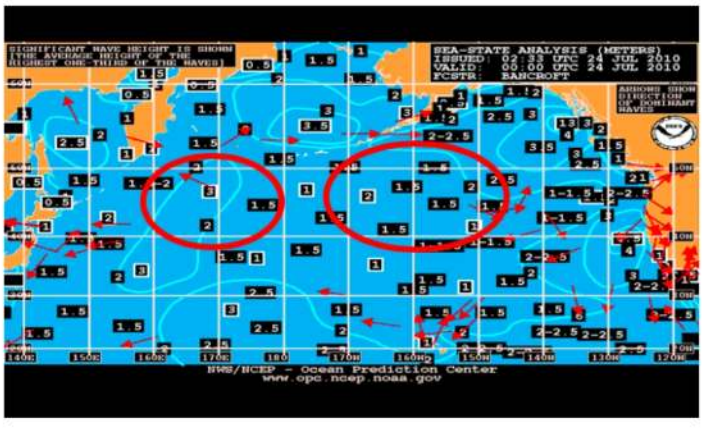

Figure 4 — NWS archival wave height chart for July 24, 2010.

actual wave heights were even lower than 1.5 m. The NWS notes state that its wave heights were calculated to warn mariners of the highest potential wave size they might encounter 48 hours in the future, and that the data for the wave height modeled predictions consider only the top one-third of wave heights likely for that period. This calculation excludes data of two-thirds of the wave heights possible, which are much lower than the 1.5 m shown on the NWS prediction chart. Sailors know that wind speeds and their resultant waves are highest during the day because the addition of solar radiation energy increases air movement, and that wind speeds drop at sunset and overnight in what sailors call the "Evening Lull." The July 24, 2010 event was at night over the darkened North Pacific. Evaluating all this in context convinced me that the NWS-modeled possible maximum wave heights under those highs likely exaggerated the actual surface wave heights between Japan and San Diego during the dark North Pacific night on July 24, 2010.

As we guessed, archived satellite coverage of the mid-North Pacific in 2010 is scanty, but my SIO classmate Gabi integrated satellite data of North Pacific wave heights near the two *PROPLAB* ocean reflection points at 2.5 hours after the July 24, 2010 propagation event. The data showed actual wave heights — "ground truth" — of between 0.77 m to 1.1 m (2.5 ft to 3.6 ft), with the majority of wave heights around 1.0 m (3.3 ft).

Eureka! That is a smooth sea for any ocean. This data confirmed that the NWS wave height prediction of 1.5 m was at least 33% higher than actual wave heights on July 24, 2010. So I believe I found some answers to what enhanced the 7 MHz CW propagation across the North Pacific on July 24, 2010 and allowed all those weak JA call signs to be copied by my San Diego *CW Skimmer*: smooth sea reflections of refracted specular and multiple diffuse scattered 7 MHz rays under North Pacific high pressure areas.

Data Checks

See **Table 1**. *VOACAP* / NWS: to be sure, I researched the 12 year period 2010 to 2021 in the NWS archives for the locations of the North Pacific highs on each July day of the JA domestic CW contests, and the highs were there each year, but not in winter where in January 2010 lows with 7 m (23 ft) wave heights and 45 kt (52 mph) took their place — rough seas! The *VOACAP* data showed only one hour of 90% 40 m propagation at 16:00Z (08:00 PST) for January compared to 5 – 6 hours in July.

RBN: I researched the RBN archives again for reported high JA spot numbers by west coast stations on the days of the July JA domestic CW contests each year from 2010 to 2021. I could find no other southern California *CW Skimmer* reports besides my own, so I relied on regular RBN 40 m reports from Robert Wilson, N6TV, in Santa Clara, CA (LAT 37° N) and Jack Reed, WA7LNW, (also LAT 37° N) in mile-high, radio-quiet Utah. Both *CW Skimmers* reported regularly over the 12 years. Of twelve month-of-July 7 MHz JA high spot count days over 12 years, six showed NWS corrected day of "*seasanal*" wave heights of 1 m or less, three of 2 m or less, two less than 3 m, with one outlier.

Ap/Kp/Wave Heights: I checked the space weather Ap/Kp indexes and wave heights for the July dates each year from 2010 to 2021. For the July high JA RBN spot dates there was a correlation with Kp index values between 0 and 1.7 (Kp range of 0 – 3) and/or NWS-reported wave heights of 2 m or less (likely corrected ground truth wave heights of 1.34 m or less), but no correlation with any Ap index values (Ap range of 2 – 15).

Conclusion

It took a decade, but I believe I've solved the mystery of the normally good, but sometimes superb, annual summertime 7 MHz propagation across the North Pacific. What I experienced on July 24, 2010, and what other western US stations experienced over 12 years, was regular good 7 MHz summer propagation across the North Pacific enhanced by the presence of the relatively smooth ocean surfaces below the regularly occurring Pacific highs. The smooth sea reflections likely reduce loss and produce composite stronger RF signals at the path end than rougher seas would produce.

Contributors

The author acknowledges and thanks RF engineer Carl Luetzelschwab, K9LA; meteorologist Jim Bacon, G3YLA, of the UK MET (ret.); EE and Oceanography Prof. Gwyn Griffith, G3ZIL, of the UK NOC (ret.); Univ. of Scranton EE Prof. Nathaniel

Table 1 – Tabular data of RBN western US-JA 7 MHz RBN spots 2010 to 2021

(a) RBN US West Coast JA Spots.

(b) Great Circle Pacific Wave Heights (NWS Maps & Satellite).

Pacific highs are present in all data.

Year	*(a) WA7LNW*	*(a) N6TV*	*(a) N6NC*	*(a) N6WIN / W6YX*	*(b) Wave Heights*	*10.7 cm SFI*	*SSN*	*A-Index AP*	*K-Index Kp1*
2010 7/24	N/A	N/A	141		0.77m-1.0m (Satellite data)	85.5	47	4	1.7
2011 7/23	172	N/A	N/A		2.5m-4.5m	86.3	43	7	2.3
2012 7/21	76	226	33		2.0m	104.6	29	8	2.3
2013 7/27	187	N/A	96		1.0m	109.3	68	9	2.7
2014 7/26	168	N/A	3		2.0m-3.0m	114.6	58	6	1.3
2015 7/25	128	N/A	N/A		1.0m	93.7	34	7	2.3
2016 7/26	58	297	N/A		1m -2m	88.9	27	7	2.0
2017 7/22	1	243	N/A		1m	90.4	0	15	3.0
2018 7/21	342	410	N/A	N6WIN, 236	2m	70.2	12	10	1.7
2019 7/20	128	115	N/A		0m-0.5m	68.3	0	2	0
2020 7/18	151	96	N/A		2m-3m	68.1	0	3	1.3
2021 7/17	269	51	N/A	W6YX , 377	1.0m	78.1	48	3	1.0

Frissell, W2NAF; Distinguished Prof. of Oceanography Lynne Talley, and Corey Gabriel, PhD JD, of Scripps Institution of Oceanography/UCSD; NOAA/Southwest Fisheries oceanographer and data analyst Gabriel Arce; EE Prof. Nozomu Nishitani of Nagoya University in Japan; Manuel Cervera, PhD, and Prof. Stuart Anderson, Adelaide Univ., consultants to Australian MOD, for their guidance, comments, research and data contributions to the final form of this article.

HL Serra, N6NC, has been a licensed amateur since 1959. He has held a USCG Master's license, served in the US Merchant Marine (1964-65) and the US Navy (1968-70) as an OOD, navigator and naval intelligence officer in Vietnam and Cambodia. He has sailed the Atlantic and Pacific Oceans, the Caribbean Sea, sailed to all the countries of the Western Pacific Rim, transited the Pacific from Japan to San Diego, and transited the Panama Canal. In 2009-2011 he quarterbacked the successful legal defense of San Diego radio amateurs against a proposed ordinance intended to prevent the erection of HF antennas in the City of San Diego. His strategy was adopted by the ARRL and serves as the template for defense against similar local measures. He retired as a practicing lawyer and law professor in 2013, and in 2016 earned a masters degree from Scripps Institution of Oceanography/UCSD, with an interest in the physical causes of meteorological and climate events. He has published articles in QST *and* NCJ *on antennas that he designed and built, and he assembled and captained the 6E2T contest team that won the 1995 ARRL DX CW Contest (DX WORLD M/2 class) from Ensenada, Mexico. Since then he contests with the NX6T team remotely to the WA6TQT Anza Radio Ranch contest station.*

References

[1] D. Day, N1DAY, "Ocean Wave Height as a Variable in Predicting HF Propagation," *CQ Magazine*, July 2017 p. 10.

[2] Junluo Li, "Reflections of the Multi-hop HF Radio on the Rough Ocean Surface," *Advances in Computer Science Research*, Vol. 87, 3rd International Conference on Mechatronics and Information Technology (ICMEIT) 2019).

[3] H. Wang, "The Study of Multi-hop HF Radio Propagation," *2019 IEEE 2nd International Conference 0n Information Systems and Computer Aided Education* (ICISCAE).

[4] Personal communication with Carl Luetzelschwab, K9LA.

[5] *Ocean Navigator Magazine* (Jan 1, 2003) **https://www.oceannavigator.com/avoiding-the-pacific-high/**.

[6] S. Taylor, "Northerly surface wind events over the eastern North Pacific Ocean: Spatial distribution, seasonality, atmospheric circulation, and forcing," PhD thesis, Scripps Institution of Oceanography / UCSD 2006, **https://escholarship.org/content/qt62x1f76v/qt62x1f76v.pdf**.

[7] S. Saito, M. Yamamoto, T. Maruyama, "Arrival Angle and Travel Time Measurements of HF Trans-equatorial Propagation for Plasma Bubble Monitoring," *Radio Science*, Vol. 53, Issue 11, p. 1304 (2018).

[8] R. Silberstein, F. Dickson, "Great Circle and Deviated-Path Observations on CW Signals Using a Simple Technique," *IEEE Transactions on Antennas and Propagation*, Vol. 13, Issue 1, p.52, (Jan. 1965).

[9] Personal communications with Prof. Stuart Anderson, Adelaide Univ., Australia.

Brian R. Callahan, AD2BA
19 Bank St., Troy, NY 12180-4303; **callab5@rpi.edu**

A First Commentary on the CW Record Protocol

A review of the CW Record Protocol with responses to suggestions, critiques, and additional features.

The CW Record Protocol **[1]** garnered a healthy amount of attention since publication. A number of amateur operators wrote to give me support, provide critique, and suggest additional features that I had not considered in my original formulation. Others expressed interest in a tangible implementation of the protocol through hardware and software.

As mentioned in the original article, follow up articles to address commentary and detail further development would be forthcoming. In this article, we will review the CW Record Protocol, introduce and respond to the three major suggestions, critiques, and additional features offered by amateur operators — who graciously took the time to respond to the original article — consider the potential pedagogical and outreach potential for the CW Record Protocol and novel protocol development writ large, and finally conclude with a look towards continued future work.

Because future work and the next major article on the CW Record Protocol will focus on a software-based implementation, the addressing of suggestions, critiques, and additional features will not necessarily make a direct attempt to refigure the protocol itself with these additions. Rather, the goal of this article is to gauge directionality of these additions and responses to them in order to guide the initial software implementation.

As with the previous article, comments, criticisms, and suggestions from the public are solicited and welcome. It continues to be my hope that these articles spur a continued interest in protocol development at all levels of complexity.

A brief review of the CW Record Protocol

Building off previous work by Intel in their HEX Record format **[2]** and Motorola in their S-Record format **[3]**, the CW Record Protocol provides two important features that enable the transmit and reception of binary data over Morse CW. First, inspired by the work from Intel and Motorola, data content is broken down into manageable chunks, known as records, that are then encoded in such a way as to reduce the time to transmit messages. Second, the CW Record Protocol provides a semi-standardized sequence of events that dictates how the data is to be transferred: stations establish communications by any agreeable method such as a routine QSO, then begin rounds of transmit, error checking, and record re-request, followed by a data termination response from the receiving station (data termination does not imply termination of communications). Stations can then continue what may be an otherwise typical QSO or terminate communications.

Suggestions, critiques, and additional features

I was fortunate enough to receive a number of comments and critiques from the original article as well as a presentation given during the August 2021 QSO Today Virtual Ham Expo **[4]**. The majority of this article will be spent addressing the three most major suggestions, critiques, and additional features discussed in those conversations. These are presented and addressed in no particular order.

Unambiguous start record characters

The first critique we will address centers around the potential fragility of relying on a specific number of dit time-units between records. Instead, it was suggested that we follow the suggestion of both Intel HEX Record and Motorola S-Records in that each begin with a character (colon in the case of Intel HEX, S in the case of Motorola S-Records) that cannot be found anywhere else in a record, and thus serves as a clear demarcation of the beginning of any record. An idea to use prosigns and/or punctuation for such a starting character was forwarded. This certainly seems like a worthwhile idea to consider and explore.

Potential downsides could be size: particularly poor choice of prosign and/or punctuation could needlessly inflate the time to transmit a message. However, there is an implicit gain to be made here as well that could mitigate at least some of that inflation penalty: we no longer need to impose a time space greater than space between words (7 dit time-units) between records, as the starting character makes the delineation for us. This saves two dit time-units between records for every record compared to the original formulation, which suggested 9 dit time-units between records. Even more, we can combine functions of the start unit character and the record type and create

single-character start signs that perform both of those functions.

Note that in the original formulation, records began with one of A0, A1, or A2. Encoded per the suggested table in the article, that produces a mandatory time to transmit overhead of 9 dit time-units for the most common A0 record (7 dit time-units for A plus 1 dit time-unit for 0 plus 1 dit time-unit for the space between characters). A1 and A2 records each have an overhead of 11 dit time-units. Combining the time between records we save and the overhead, we can stand to improve efficiency.

We might also note that there are a plethora of letters that go unused in the CW Record Protocol and we could in theory use these letters as the start characters. I am, however, keen to avoid such an implementation because of the possibility that unused letters carry the potential to be less clear than characters outside the 26 letters and 10 numbers. This possibility of reduced clarity may not matter so much to computer-aided transmit and receive, and I am open to a computer-only variant of the CW Record Protocol in which maximum efficiency can be eked out through such a substitution.

For a more general use case, we can turn to punctuation marks and miscellaneous signs to take on the role of start characters. International Morse code provides for enough of these marks and signs sufficient for the CW Record Protocol and provides significant room for growth should the protocol expand far beyond its current formulation.

Table 1 provides a list of punctuation marks and miscellaneous signs, section 1.1.3 of Recommendation ITU-R M.1677-1 **[5]**, along with their dit time-units to transmit. As in the original article, dit time-units to transmit includes intra-Morse character spacing.

Immediately, the invitation to transmit and multiplication signs are eliminated as a potential start character choice; they are simply letters and as we just discussed it might be beneficial to not employ unused letters to avoid potential loss of clarity. It is even worse in the case of invitation to transmit, as K is one of the letters used for encoding in the CW Record Protocol.

Next on the potential list would be Understood ($\overline{SN}$) and Wait ($\overline{AS}$). According to the ARRL Operating Manual, Understood is a valid response to Wait **[6]**. And they are both only 11 dit time-units to transmit. For a computer-only variant of the CW Record Protocol, these might well be the winning combination to replace A0 and A1 records (A2 records, data without checksum records, would not need replacement in a computer-only variant).

My preference in the general case is for the double-hyphen character to replace A0, the cross character to replace A1, and the question mark to replace A2. Both the double-hyphen and the cross are 13 dit time-units, while the question mark is 15. Each of these special characters are symmetrical in their keying; symmetry being known to be a characteristic preferred by humans and other animals **[7]**, **[8]**, **[9]**. Hopefully symmetrical start characters aid at least slightly in their memorization in the event of human transmit and/or receive. Even in the case of computer-aided transmit and receive, the additional time between 11 dit time-units and 13 dit time-units is not so large as to be overly detrimental to the overall efficiency of the protocol.

Table 1 - Dit time-units to transmit punctuation marks and miscellaneous signs.

Sign name	*Morse equivalent*	*Dit time-units to transmit*
Full stop (period) [.]	•–•–•–	15
Comma [,]	––••––	19
Colon or division sign [:]	–––•••	17
Question mark [?]	••––••	15
Apostrophe	•––––•	19
Hyphen or dash or subtraction sign [–]	–••••–	15
Fraction bar or division sign [/]	–••–•	13
Left-hand bracket (parenthesis) [(]	–•––•	15
Right-hand bracket (parenthesis) [)]	–•––•–	19
Inverted commas (quotation marks) [“ ”]	•–••–•	15
Double hyphen [=]	–•••–	13
Understood ($\overline{SN}$)	•••–•	11
Error (eight dots)	••••••••	15
Cross or addition sign [+]	•–•–•	13
Invitation to transmit [K]	–•–	9
Wait ($\overline{AS}$)	•–•••	11
End of work ($\overline{SK}$)	•••–•–	15
Starting signal ($\overline{CT}$)	–•–•–	17
Multiplication sign [×]	–••–	11
Commercial at [@]	•––•–•	17

Address information

The baseline Intel HEX Record format affords four characters of address information in a record, yielding the entire range of the 16-bit address space (0x0000 to 0xFFFF). There are two additional Intel HEX Record types that can provide for a larger address space. The first is the Extended Segment Address, which can provide for 20-bit addresses; this somewhat curious choice of address size is a historical remnant of the Intel x86 segmented address model, which could address up to 1 megabyte of memory (20-bit addresses) divided into 64 kilobyte segments. The second is called the Extended Linear Address record type that allows for 32-bit addressing. Motorola S-Record format provides for a variable number of characters to represent an address. S1 records provide four characters and is analogous to Intel HEX, S2 records provide six characters for 24-bit addresses, and S3 records provide eight characters for 32-bit addresses.

No Intel HEX Record nor any Motorola S-Record type provides a mechanism for 64-bit addresses, which would be necessary for the majority of modern CPUs. The CW Record Protocol, in recognizing that addresses may not be necessary for modern computers and in perhaps an overzealous quest for shorter records, omitted the address field entirely. As a result, the original formulation required the transmitting station to send the entirety of the data message in order without breaks. A couple of amateur operators critiqued this design approach.

While literal addresses may not be as useful as they once were, sequence numbers may provide a more modern and robust solution to alleviate the raised issues. Sequence numbers are a solution used in packet-based networking protocols such as TCP. There are some additional benefits to sequence numbers as well. Records can be sent out of order and records could be sent over multiple transmissions if interruptions

made continuing impossible. Sequence numbers also make it easier for the receiving station to re-request bad records as one may be able to easily figure out which records are missing/malformed by keeping a list of good records and their sequence numbers, and simply re-requesting the sequence numbers for all records not on that list.

The Motorola S-Record format has additional record types, S5 and S6, that give the number of records transmitted at the end of a transmission. Such information might prove prudent as well for the CW Record Protocol, though embedding that information into an end-of-transmission record might be more suitable.

Error checking and correcting

The final primary critique of the original formulation of the CW Record Protocol is in error checking. Building off the Intel HEX record and Motorola S-Record formats, both provide for only rudimentary error checking through a checksum byte located at the end of each record. While even a single checksum byte will perform its job admirably, such a solution suffers from a number of drawbacks: perhaps most importantly, a single-byte checksum has a high probability of failure. That is to say, it is possible for many different combinations of record data to produce the same single-byte checksum. In certain instances, there is no way to distinguish between a valid record and an invalid record if both happen to produce the same checksum. With the entire range of possible checksum byte values as small as 256 as in the original formulation of the CW Record Protocol, there is ample opportunity for a deliberate attack or even random chance to cause an invalid record to be accepted as valid.

There are a few methods to deal with this issue. The first would be to simply increase the number of checksum bytes at the end of each record. Of course, this increase comes at the cost of enlarging every record. The probability of failure may still be too high. Adding just one more byte to the checksum only slightly decreases the probability of failure, still likely uncomfortably common for certain scenarios, as the range of possible checksum values increases to just 65,536. Worse still, a station determined to sabotage a communication is very likely to discover records that produce the same checksum. With such attacks being known against much more sophisticated hashing algorithms such as MD5 **[10]**, the possibility of a similar malicious attack is all too welcoming against such a simple algorithm as found in the CW Record Protocol.

The next level up in error checking sophistication would be to introduce Hamming codes. As I discussed in the article on DataTV **[11]**, Hamming codes are capable of not only detecting one-bit errors, they are also capable of correcting one-bit errors. Alternatively, one could detect two-bit errors while losing the ability to correct one-bit errors **[12]**.

These improvements come at a cost. It requires sending more data to detect and correct errors. The most basic Hamming code, Hamming(3,1), is the worst in terms of the amount of additional data required to send in order to achieve error correction, as Hamming(3,1) requires you to send three complete copies of the data; or, inversely, only one-third of all data sent is actually used to convey the intended information. Moving up to the next Hamming code, Hamming(7,4) improves this ratio to four-sevenths. Going further up continues to improve the ratio at the cost of complexity to implement. An ideal balance will be found by continued development and usage of the CW Record Protocol. Of course, additional error correcting codes exist, to pick just one additional example, Reed-Solomon codes. Further research will investigate the trade-offs for other error correcting codes.

Lastly, some recent amateur radio research can augment error correction in the CW Record Protocol in the situation where the transmitting station is able to be heard by many potential receiving stations. In this scenario, a protocol known as Packet Compressed Sensing Imaging (PCSI) may be used in order to increase the likelihood of successful transmission. PCSI, originally presented at the ARRL/TAPR 2020 conference, describes the ability for receiving stations to form an ad-hoc network that allows them to effectively pool their received transmissions **[13]**. So long as every record in a transmission is successfully received by at least one station in the network, all receiving stations in the PCSI network, through the pooling of correctly received records, will be able to fully reconstruct the message at each receiving station.

Pedagogical and outreach potentials to be found in protocol development

One-way transmissions are permitted to assist in learning International Morse code. Unfortunately, that does not actually free operators from the requirement to establish a QSO prior to sending a data transmission using the CW Record Protocol. However, there is no requirement that an additional number of stations may not *listen* to such a transmission. As such, stations are free to listen to any transmission that utilizes the CW Record Protocol and take for themselves a copy of the data being transmitted. In addition, a PCSI or PCSI-like network can therefore be established in the event that a CW Record Protocol transmission of interest is set to begin at a future known and scheduled time, and that transmission follows all the FCC rules. So it is possible in theory to obtain a data broadcast, though perhaps only with creative reinterpretation of the rules.

This creative reinterpretation paves the way for a re-creation of novel forms of data transmission pioneered in the 1980s: and discussed in a previous article **[14]**: usage of television and radio broadcasts to transmit computer data, as found on the BBC **[15]**, Swedish Radio **[16]**, German broadcasts **[17]**, the Netherlands **[18]**, and Yugoslavia **[19]**. Combined with my previous articles on SSTV **[11]**, **[14]**, The CW Record Protocol sits on the precipice of producing part of the next generation of work for amateur radio at large. No longer, in the case of CW, being simply guardians of the past, amateur radio can be poised to steward new futures for these old technologies.

I imagine using the CW Record Protocol as one of many outlets to demonstrate to the next generation of young amateur operators new ways of sharing the lives they live in the mediums and forms they are comfortable with and used to sharing their lives in, just using the technologies amateur radio stewards as the backbone of those communications, providing a vehicle through which our social media-driven lives can be better understood technically. The pedagogical and outreach potentials for these reinterpretations are vast. More such reinterpretations are needed and welcome.

The addition of pedagogic and outreach value as a focus for the CW Record Protocol, and my extended research interest in protocol development, stems from conversations with David Kazdan, AD8Y, at Case Western Reserve University, who introduced me to Coherent CW **[20]**. Kazdan uses Coherent CW in his university teaching as a part of his responsibilities as faculty advisor for the Case Amateur Radio Club, W8EDU, as Coherent CW provides a novel data mode for Technician-class license holders. It is my hope that

future articles detail collaboration between students at my home university, Rensselaer Polytechnic Institute, and Case Western Reserve University, and hopefully many others, through a shared interest in novel protocol development and other amateur radio interests that draw on and demonstrate this idea of stewarding new futures for old technologies and the pedagogical and outreach potential of the idea.

Future work

Subsequent articles will continue to refine the CW Record Protocol as additional feedback is provided and iterated upon through experience with increased usage.

A follow-up article will introduce software that provides all necessary functions to operate as a standalone computer-aided transmit and receive package. Feedback from this article and previous discussions of the CW Record Protocol will be instrumental in the ultimate formulation of this initial software package.

Security concerns may still arise in certain environments. While certain strategies exist to mitigate some potential security concerns, like outright impersonation, other security concerns are not able to be mitigated. Notably, since FCC rules forbid encryption **[21]**, amateur radio is a poor medium for information that truly needs to remain confidential. Security, then, should focus on integrity and availability where possible. Beginning with the discussion of error checking in this article, future work will include a determination of the overall trade-offs for different error checking and error correcting techniques.

Conclusion

This article investigated the three primary suggestions, critiques, and additional features for the CW Record Protocol as guided by feedback provided to the author from interested amateur operators in response to the original CW Record Protocol article. The suggestions addressed include unambiguous start record characters to help clarify how to separate records in a transmission without relying on potential unclear spacing rules; using sequence numbers for information about record ordering to facilitate reconstruction after receive, permit more accurate resend requests, and allow for records to be sent out of order and over multiple transmit sessions; and improved error detection and error correction that go beyond a simple one-byte checksum.

The article then considered pedagogical and outreach potentials for novel protocol development writ large, focusing on the idea that protocol development can add a new mission for amateur radio: stewarding new futures for old technologies.

It continues to be my hope that these articles spur continued, renewed, and fresh interest in novel protocol development at all levels of complexity. Feedback from the public is desired and appreciated to help guide future work.

Acknowledgments

I would like to thank all the amateur operators who provided feedback and conversation about the CW Record Protocol and other protocol development topics, including but not limited to David Kazdan, AD8Y; Rick Peterson, WA6NUT; John Tarbox, WA1KLI; Randy J. Richmond, W7HMT; George Mallard, KC5LPK; and David Underwood, KØIMH. A mailing list for amateur operators interested in protocol development topics has been set up at **https://groups.google.com/g/hampro-list**.

Brian Callahan, AD2BA, is an Amateur Extra class license holder. He earned his PhD at Rensselaer Polytechnic Institute and currently serves on the faculty of the Information Technology & Web Science program, also at RPI, where he conducts research into cyber security pedagogy and digital humanities, and teaches courses in cyber security and web science.

Works Cited

[1] B. R. Callahan, "Protocol for Formatting and Transmitting Binary Data over Morse CW." *QEX* May/June 2021, pp. 31-33.

[2] Intel Corporation, "Hexadecimal Object File Format Specification: Revision A." 1988 see: **https://archive.org/details/IntelHEXStandard/mode/2up**.

[3] Lucid Technologies, "Motorola S-record Format," see: **https://www.lucidtechnologies.info/moto.htm**.

[4] B. R. Callahan, "Design your own communication protocols," QSO Today Virtual Ham Expo August 2021 see: **https://www.qsotodayhamexpo.com/player-august.html?link=NTk0ODM2NTQ0**.

[5] International Telecommunication Union, "Recommendation ITU-R M.1677-1: International Morse Code," 2009, see: **https://www.itu.int/dms_pubrec/itu-r/rec/m/R-REC-M.1677-1-200910-I!!PDF-E.pdf**.

[6] *ARRL Operating Manual* (10th ed.), 2012, Newington, CT: American Radio Relay League.

[7] M. Enquist, A. Arak, et al., 1994. "Symmetry, beauty and evolution." Nature 372: 169-172.

[8] A. C. Little & B. C. Jones. 2003. "Evidence against perceptual bias views for symmetry preferences in human faces." Proceedings of the Royal Society of London. Series B: Biological Sciences 270: 1759-1763.

[9] R. Reber, N. Schwarz, & P. Winkielman. 2004. "Processing fluency and aesthetic pleasure: is beauty in the perceiver's processing experience?" Personality and Social Psychology Review 8(4): 364–382.

[10] P. C. van Oorschot, and M. J. Wiener. 1999. "Parallel Collision Search with Cryptanalytic Applications." Journal of Cryptology 12: 1-28.

[11] B. R. Callahan, "DataTV: A protocol for embedding data into SSTV transmissions." *QEX,* March/April 2022, pp, 25-28.

[12] R. Hamming, 1950. "Error Detecting and Error Correcting Codes." The Bell System Technical Journal 29(2): 147-160.

[13] S. Howard, G. Barthelmes, C. Ravasio, L. Huang, B. Poag, and V. Mannam. 2020. "Packet Compressed Sensing Imaging (PCSI): Robust Image Transmission over Noisy Channels." ARRL/TAPR DCC Proceedings, 2020. Online: **https://files.tapr.org/meetings/DCC_2020/2020DCC_Howard.pdf**.

[14] B. R. Callahan, "Experiments in gaming over SSTV", *QEX,* July/August 2022, pp. 25-30.

[15] BBC, "*Tomorrow's World* - Computer program transmitted over TV." see: **https://www.youtube.com/watch?v=jeKWMXuSGCc**.

[16] J. Wilhemsson, "Sveriges Radio fildelade redan på 1980-talet." 2014, see: **https://techworld.idg.se/2.2524/1.562426/sveriges-radio-fildelade-redan-pa-1980-talet**.

[17] "r@dio.mp3 - Stadtwiki Karlsruhe," see: **https://ka.stadtwiki.net/R@dio.mp3**.

[18] T. English, "You Could Download Video Games From the Radio in the 1980s." 2020, see: **https://interestingengineering.com/you-could-download-video-games-from-the-radio-in-the-1980s**.

[19] B. Jakic, "Galaxy and the New Wave: Yugoslav Computer Culture in the 1980s." 2014. In *Hacking Europe: From Computer Cultures to Demoscenes.* G. Alberts and R. Oldenziel, eds. Springer: London. pp. 107-128.

[20] R. C. Petit, "Coherent CW: Amateur Radio's New State of the Art?" *QST* Sep. 1975: 26-27.

[21] 47 CFR § 97.113 - Prohibited transmissions: **https://www.law.cornell.edu/cfr/text/47/97.113**.

Benjamin Neveu
Lieu dit Chantepie 72330, Cerans Foulletourte, France; **ben.neveu.2704@gmail.com**

SSB Receiver Controlled by a Smartphone

This approach saves cost by using the smartphone for a display and for control.

As a student in IT at Touchard Washington High School in Le Mans, I carried out a 6 week internship at the F6KFI Radio Club of Le Mans. My internship topic was to program a human-machine interface (HMI) of an SSB receiver based on the SI4735 integrated circuit. Typically, this component, which costs only a few dollars, is driven by an Arduino and a touch screen. My program aims to control the receiver with a simple smartphone. This reduces the cost, since the complete receiver is reduced to an ESP32 microcontroller with a Wi-Fi access point and the SI4735.

The SI473x Integrated Circuit

The SI4735 consists of two antenna inputs followed by two amplifiers. The IQ demodulator as well as the analog to digital converters are well recognized. The signal processing is done directly internally by the Digital Signal Processor (DSP). The signal is sufficient to drive headphones directly from the audio outputs ROUT and LOUT to hear the selected station.

Four receiver bands are supported:

- 87 – 108 MHz: classic FM reception with RDS decoder,
- 153 – 279 kHz,
- 520 – 1710 kHz,
- 2.3 – 26.1 MHz.

SSB reception is made possible by a micro code downloaded into the SI7435 at power on. The integrated circuit works in the same way as a classic Software Defined Radio (SDR) receiver without the need for a computer. The selection of the reception frequency and the reception mode are done by a microcontroller via an I²C bus. The

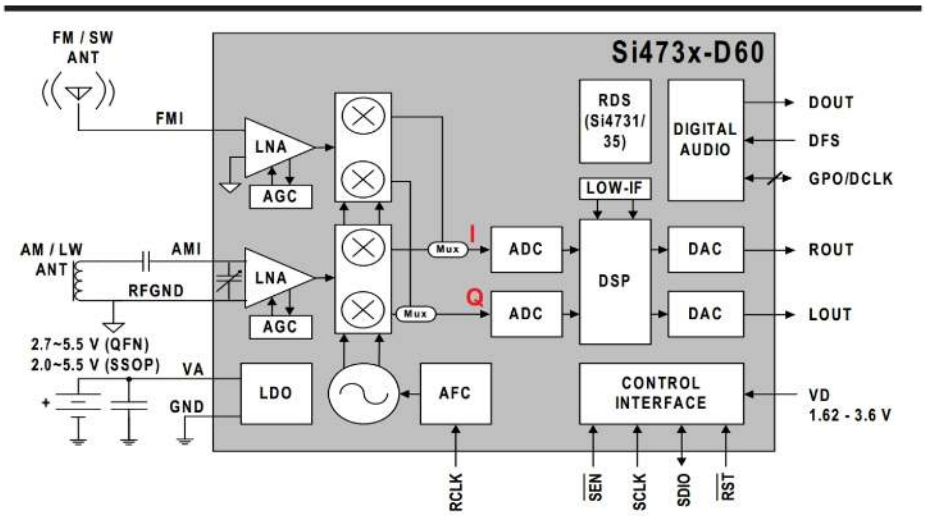

Figure 1 — Internal block diagram of the SI4735.

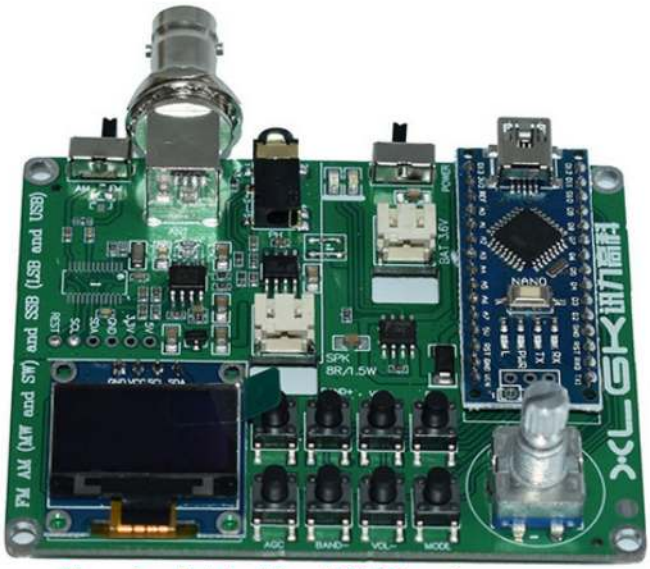

Figure 2 — Arduino kit and SI4732 receiver.

microcontroller does not perform any audio processing, it is only used to control the SI4735 and to host the web page, which is the control interface of my project. The local oscillator is clocked by a 32,768 Hz quartz crystal. **Figure 1** shows the internal block diagram of the SI4735.

Existing Kits

Kits with a SI473x can be found on the internet. As seen in **Figure 2**, the SI4732 based receiver is driven by an Arduino Nano. Moreover, the OLED screen is too small, and the set lacks flexibility in use; it is impossible to enter a frequency directly.

There are many other projects still based on the Si473x integrated circuit. Ricardo Caratti, PU2CLR, has made a library **[1]** specially designed for the SI473x. He also lists various projects on his site, such as the receiver driven by an ESP32 and a TFT touch display ILI9341 (**Figure 3**). This one offers a certain comfort in the readability, but the cost of the display is not negligible.

The Objective of My Project

The objective is very simple: control the receiver with a smartphone instead of a display. For this, I must design an HMI using a Wi-Fi access point and a web page. It would have been possible to make a dedicated application for Android, but using a web server directly integrated in the ESP32 microcontroller allows for a more versatile use of different brands of smartphones.

As a result, the hardware parts count is reduced to the bare minimum (see **Figure 4**):

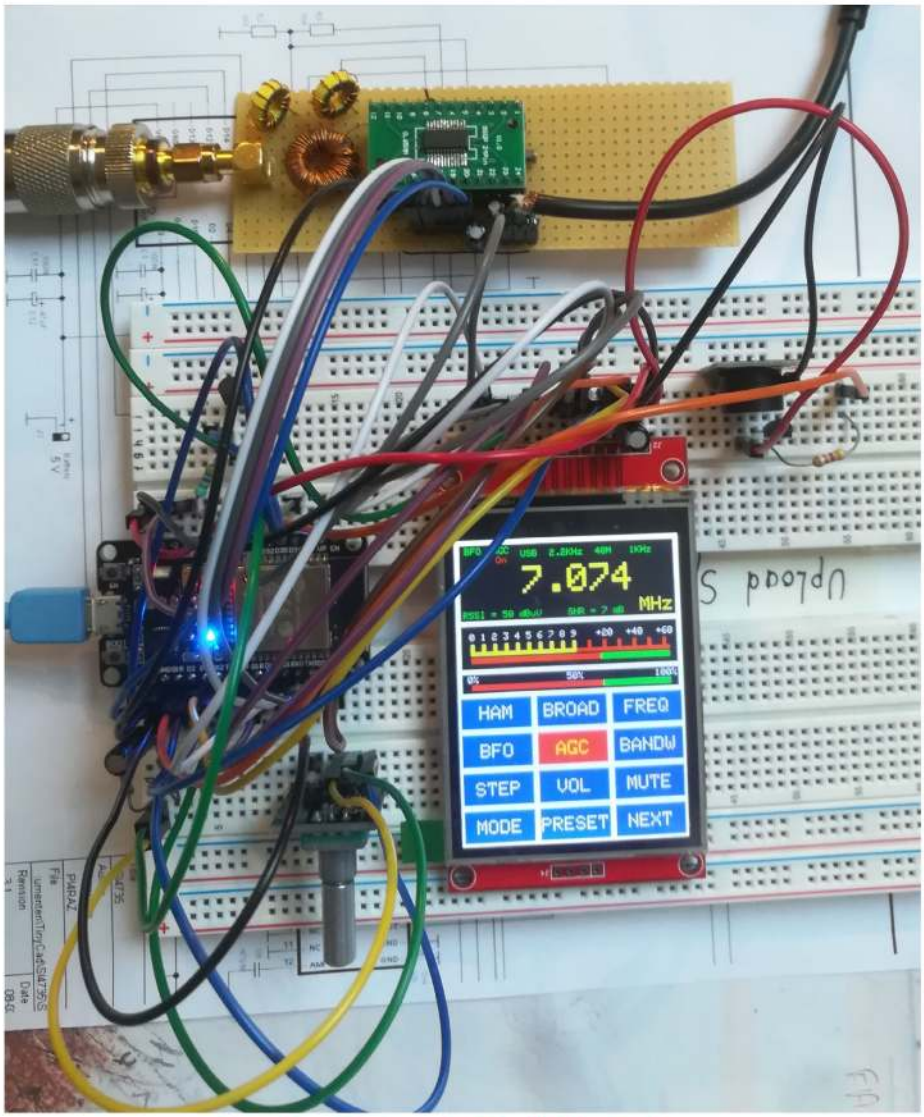

Figure 3 — Breadboard with an ILI9341 display.

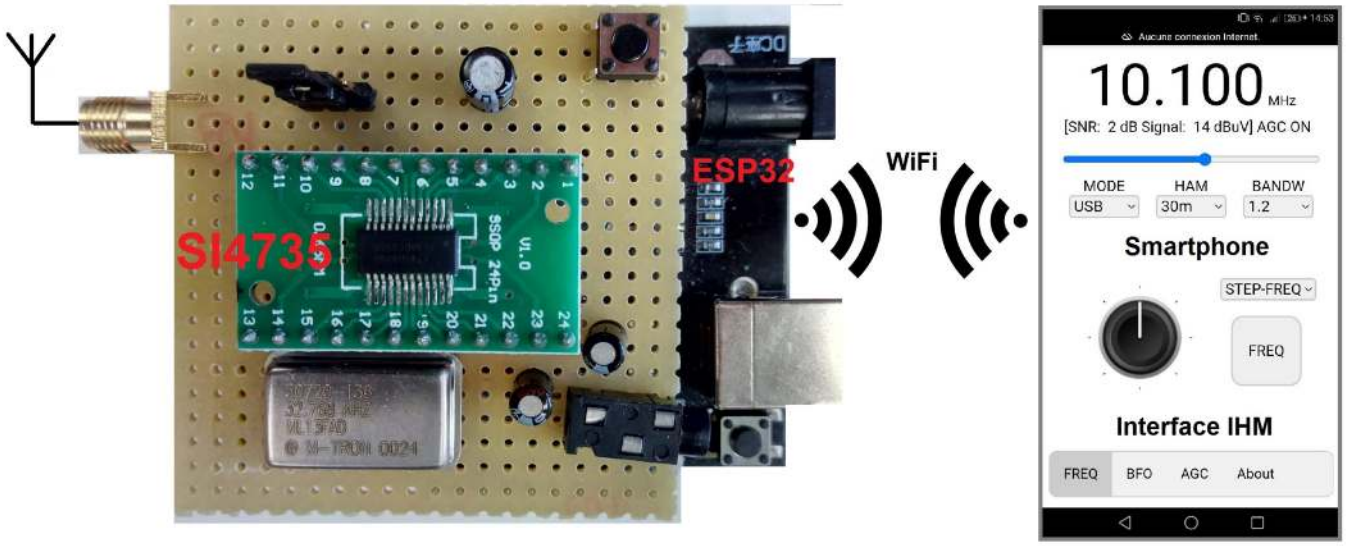

Figure 4 — Prototype using a smartphone.

Figure 5 — Human Machine Interface.

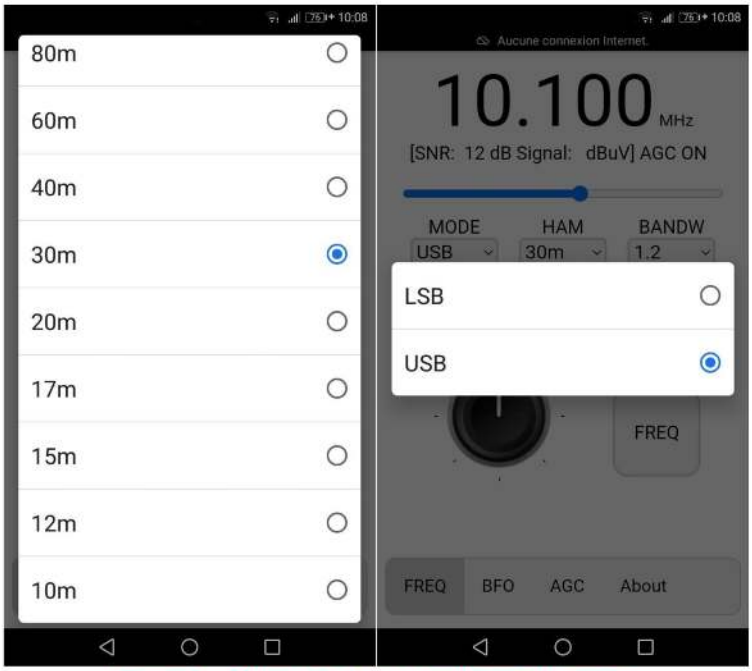

Figure 6 — Selection of bands and reception mode.

- An ESP32.
- A SI4735 with its 32,768 kHz quartz crystal.
- A wide band HF filter at the input.

Benefits of Using the ESP32

There are a lot of projects based on the ESP32 microcontroller on the internet. It has a 2-core SoC clocked at a frequency of 240 MHz, 4 MB of flash memory, and 520 KB of RAM. Wi-Fi connectivity and Bluetooth are integrated into the circuit. These are the strong points of this microcontroller as any connected object. The Wi-Fi access point managing the Web server is realized by the ESP32 and has nothing to do with the internet network. It is possible to use the receiver in a portable station configuration.

In an atMega328p (Arduino Nano) it would have been impossible to fulfill this objective because it has no Wi-Fi connectivity and has a very limited memory.

Interface Description

The programming was done with the Arduino IDE and NetBeans **[2]** in C++. The web page uses JavaScript code and automatically dialogues with the ESP32 acting as an interface between the smartphone and the SI4735 receiver. The user has only one web page with different tabs. The description follows the ESP32_SSB.ino file, in the ESP32_SSB folder, in the 01_Projets folder of the ESP32_Si4735_Control_by_WiFi-master.zip file on **www.arrl.org/QEXfiles**.

Figure 7 — The "About" tab.

In the upper part of the HMI (**Figure 5**), we find the main information:

- Frequency,
- Signal to noise ratio (SNR),
- The RSSI (Received signal strength indicator),
- The status of AGC on or off,
- A slider for volume control.

Just below (**Figure 6**), there are three drop-down lists that allow you to choose the mode (LSB, USB), the different bands (10 m to 630 m), then the bandwidth in BANDW listening (0.5, 1.0, 2.2, 3.0, 4.0 kHz).

- The "FREQ" tab is composed of a rotary knob which is reminiscent of the one present in any conventional receiver. This one allows you to increment or decrement the frequency with a step that you can select right next to it in the "STEP-FREQ" drop-down list (1 kHz, 5 kHz), the "FREQ" button allows you to directly enter the frequency you wish to listen to.
- The "BFO" tab has the same elements as the "FREQ" tab. This allows you to adjust the frequency more precisely according to the step selected via the "STEP-BFO" selection (1 Hz, 5 Hz, 10 Hz, 25 Hz). The "Reset" button allows you to reset the BFO setting.
- The "AGC" tab allows you to activate or deactivate the automatic gain control.
- The "About" tab displays (**Figure 7**) the author of the program.

How to Implement the Project?

I have created a Github site **[3]** indicating the programming procedure. A printed circuit board (**Figure 8**) will be available soon, and the board production files are on the **QEXfiles** web page along with additional images, schematics, and software.

Conclusion

The internship at the F6KFI Radio Club was very enriching for me. I was able to apply all the computer science courses (C++,

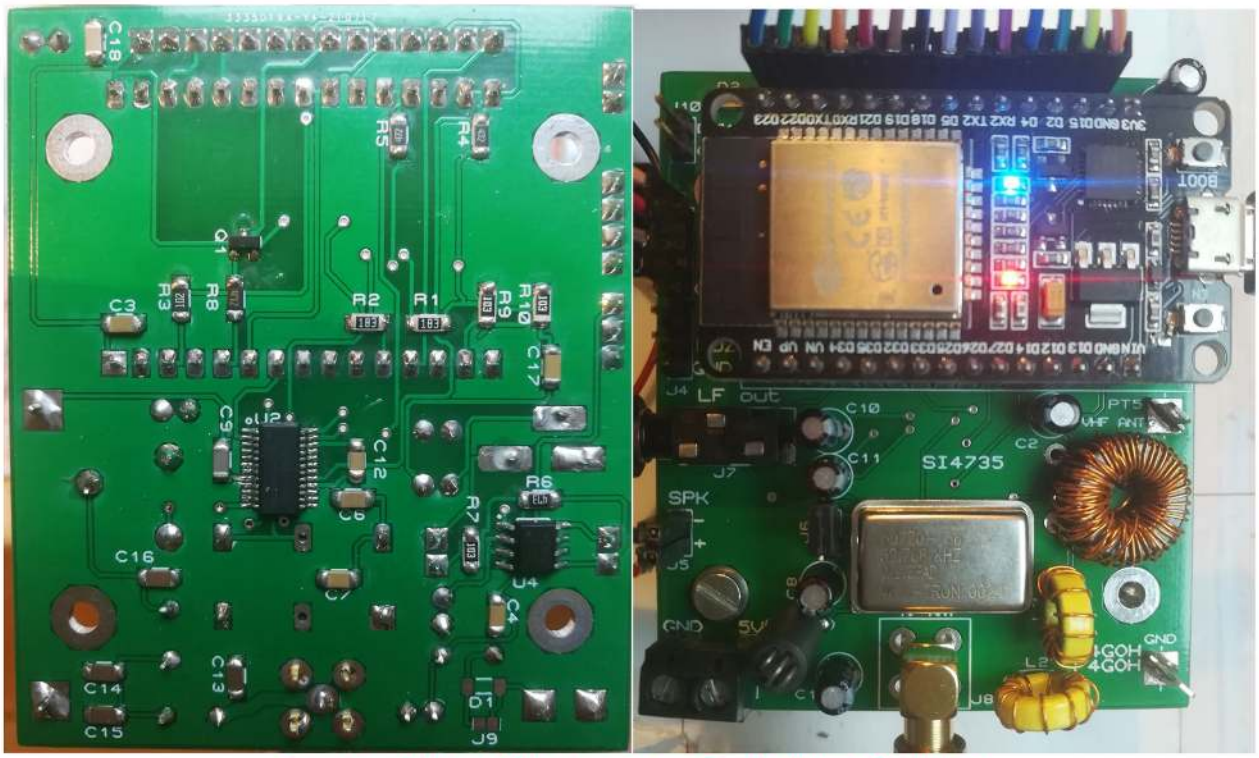

Figure 8 — Prototype SSB receiver board Front (right) and Back (left).

HTML, JavaScript) acquired during my first year of BTS at Gabriel Touchard - George Washington High School through the SSB receiver project. I thank Mr. Ghislain Ballester, F4HGA, president; Mrs. Christine Carreau, F4GDI, vice-president; and Mr. Anthony Le Cren, F4GOH/KF4GOH, member and teacher at the Touchard High School, to have welcomed me to the Radio Club. I also thank teachers Mr. Simier, Mr. Cruchet and Mr. Bernard at Touchard High School for the help they gave me during my training **[4]**.

Benjamin Neveu currently attends a two-year post-A-level in IT at Touchard High School in Le Mans, France. He is a shortwave listener, and plans to take the amateur radio license exam soon. His internship at the F6KFI Club enabled him to discover the different modes of transmission and to implement them through a Human Machine Interface. Benjamin observes that computer science is more and more present through SDR receivers.

Notes

[1] Ricardo Caratti, PU2CLR, library: **https://github.com/pu2clr/SI4735**.
[2] Install Arduino IDE: **https://github.com/PhilippeSimier/Esp32/tree/master/00_install_EDI**.
[3] Programming: **https://github.com/BenjaminNeveu/ESP32_Si4735_Control_by_WiFi/tree/master/EN**.
[4] Public workspace: **http://touchardinforeseau.servehttp.com/ent/public/**.

Errata

Dear Editor,

In "Self-Paced Essays #11: Reactance," by Eric Nichols, KL7AJ, the statement "we use j Im{Z} to indicate the reactive or imaginary part of the impedance" is not correct; the imaginary part of the impedance is Im{Z} without the j. Additionally, the correct expression for capacitive reactance using the author's sign convention should be $X_C = -1/(2\pi f C)$. There are two conventions to specify reactance, and in the convention used by the author, a minus sign is missing. These matters are discussed in textbooks on circuit theory and analysis, and in IEEE standard definitions [IEEE Standard 270-2006, 3.266 and 3.267] and [The Authoritative Dictionary of IEEE Standards Terms, 7th Edition, *Institute of Electrical and Electronics Engineers*, 2000, p. 929. ISBN 0-7381-2601-2]. — *Phil Erickson, W1PJE,* **phil.erickson@gmail.com**; *William Liles, NQ6Z; Steve Stearns, K6OIK.*

Author Nichols responds,

I missed that in my final review. Thanks for the note! George Grammar, W1DF, in his August 1943 *QST* article, as well as other ARRL publications, use the positive convention of capacitive reactance. — *Eric Nichols, KL7AJ*, **kl7aj72@gmail.com**.

The Editor replies,

Reactance is indeed Im{Z} without the j. Grammer's August 1943 *QST* article does call out capacitive reactance as a positive quantity, as do other ARRL publications. For consistency with Nichols' text and Figure 1, the negative sign convention applies here. In their letter, Phil Erickson, W1PJE, et al., also point out this choice, while mentioning that there are two conventions. In a subsequent letter, Larry Joy, WN8P, supports the choice with the minus sign. — *73, Kai Siwiak, KE4PT, QEX Editor.*

Errata – *QEX* July/August 2022

In the *QEX* article "Multi-Band HF Phasing Receiver Using SoftRock Ensemble II and Arduino Uno," by Dave Harrison, W6IBC, we erroneously identified Rick Campbell's call sign as NN7B in several locations. In fact Rick's call sign is KK7B. We regret the error

Errata – *QEX* July/August 2022

In the *QEX* article "Self-Paced Essays #12: Resonance," by Eric Nichols, KL7AJ, the correct expression for capacitive reactance magnitude on p. 34 should be $|X_C| = 1/(2\pi f C)$. Also on p. 35 in three places, as well as in the formula for Z, X_C should be $|X_C|$. We regret the errors.

Eric P. Nichols, KL7AJ

AlasKit Educational and Scientific Resources, 3763 Lyle Ave., North Pole, AK 99705; **kl7aj72@gmail.com**

Self-Paced Essays — #13 Parallel Complex Circuits

Parallel reactive and resistive components can be solved graphically and by formulas.

We trust you have had a chance to ponder the last essay's parting question: is the capacitor in series with the inductor, or in parallel? The answer is that there's not enough information to answer the question! It only becomes meaningful when we consider where we connect the power source. If we break the loop and insert a voltage source in the loop, it's a series circuit. If we leave the circuit as is, but put a power source in parallel with the existing components, it now becomes a parallel resonant circuit. We can't actually put a true voltage source directly across the circuit, because a true voltage source would short out the circuit, so we need to put a high value of resistance in series with our generator. This becomes a "pseudo-current source" — sometimes called a dependent or controlled current source. A true current source (independent current source) puts out the same current no matter what, which would cancel out what we need to demonstrate so, instead we will use a voltage source and a high value of series resistance (**Figure 1**)

As in our previous series resonant example, this circuit is tuned to 5.033 MHz, with a frequency sweep between 4.5 and 5.5 MHz. We will plot the current through R1 and the current through L1, which will be the same as the current through C1, but in the opposite direction (**Figure 2** and **Figure 3**).

So, how do you explain this behavior? Well, you either believe Kirchhoff's Current Law (KCL) or you don't! Let's look at the

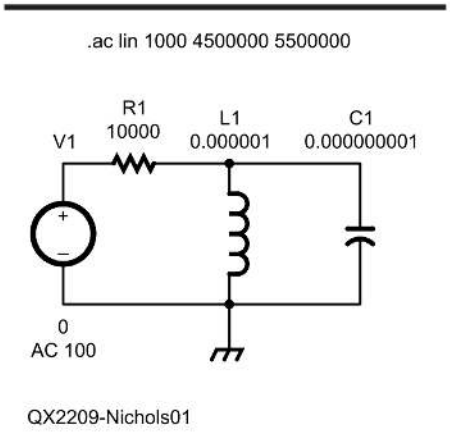

Figure 1 — A parallel resonant circuit.

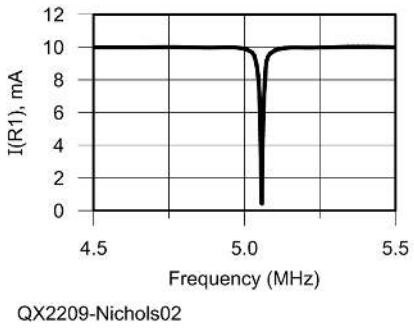

Figure 2 — Current through R1.

SPICE node junction between R1, L1, and C1. Let's assume there is no resistance inside the loop. At resonance we would have infinite current circulating, or more aptly, "sloshing back and forth" between L1 and C1. Well, in the real world we won't have zero internal loss, but it can be very, very low. At any rate, KCL tells us that the current entering the node has to equal the current leaving the node. If at any time the current emerging from L1 into the node is equal to the current leaving the node and entering C1 (or vice versa), there is no possibility of current entering the third port of the node, the port where R1 is connected. At resonance, the L1 and C1 currents will be equal and opposite, and so R1 current will be minimum.

As always, we encourage you to actually build this circuit and make some measurements; don't rely entirely on *SPICE* modeling. However, I've never encountered a properly modeled *SPICE* program that didn't very closely match reality.

The parallel tuned "tank" circuit is actually a special case of countless complex parallel circuits, but it's an important one. We will come back to visit this with a great deal more detail, later on.

Back to Basics, Sort of

Being able to work out complex series circuits is fairly straightforward. If you know the Pythagorean Theorem, you can work these problems out in minutes, or sometimes in your head. However, when dealing with parallel components, the calculations can be a bit more "fun."

Let's say you have a 100 Ω resistor and 50 Ω of inductive reactance in parallel with the resistor. We want to know the

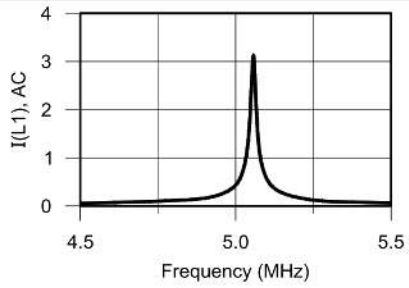

Figure 3 — Current, amperes, through L1 or C1

SPICE Modeling with Current Sources

We hope some of you have had a chance to experiment with *SPICE* circuit modeling. It's a wonderful way to learn a lot of circuit principles. There are a few cautions and quirks about *SPICE* that you should know about. Probably the one that causes the most confusion to novices is how it handles current sources.

Current sources in *SPICE* are independent current sources. That is, they put out a finite, fixed amount of current regardless of what they're connected to. This is a crucial component of differential amplifiers, and operational amplifiers in general, which we will discuss in great detail before too long. *SPICE* was indeed created primarily to assist in the design of such active circuits.

However, if you try to model, say, a parallel tuned circuit driven with a *SPICE* current source, you will get no results, or very odd ones.

What you need for these situations is a dependent current source, which is a voltage source and a high value of resistance in series. That is precisely what we do to model most parallel tuned circuits.

Incidentally, this also applies to current sources in *NEC* antenna modeling. Until fairly recently, most "front ends" to *NEC* modeling did not offer current sources at all; the user had to "manufacture" them from the normal voltage sources. Now, most *NEC* "flavors" include an ideal current source. We will explore *NEC* antenna modeling before too long, as well.

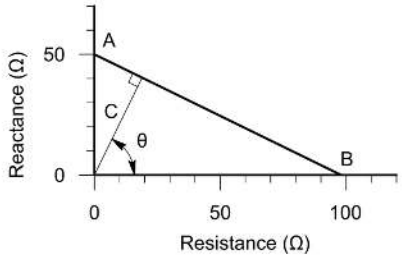

Figure 4 — Parallel impedance graphic solution.

total impedance. Remember, we always want our answer to have both magnitude and phase. How do we go about solving this? There is a neat graphical solution to this, which I learned in a slide rule manual. Interestingly enough, I've never seen this method described in any textbook, either amateur or commercial; I don't know why this was not published far and wide. However, I have checked it out thoroughly, and it always works. So, I will happily pass along this privileged information. Perhaps, as an exercise, one of you can explain exactly why it works, see **Figure 4**.

First plot your reactance at Point (A). Plot your resistance at Point (B). Draw a segment between points A and B. Now draw another segment C from the origin to segment AB, where the new segment is perpendicular to segment AB. The length of segment C is the impedance magnitude, and the angle θ, shown in the plot, is the phase angle. All you need is some quadrille paper, a straight edge and a protractor. Pretty tricky, eh?

Now, in case you aren't safe around pointy objects like pencils and compasses and other drawing paraphernalia, we can solve this with mathematics. For a parallel resistance and reactance, the formula for impedance magnitude $|Z|$ is:

$$|Z| = \frac{|RX|}{\sqrt{R^2 + X^2}} .$$

The formula for phase angle is:

$$\theta = \arctan\left(\frac{R}{X}\right) .$$

For the values given, the impedance magnitude is 40.0 Ω. The phase angle is 60°. You might want to practice a few times with a ruler and a protractor on a few problems and see how close you come to your calculator's answer. Later on, we'll use another graphical method, namely the Smith Chart, to figure out both impedances, and their reciprocal values, admittances.

In our next essay we'll talk more about Q, and various methods of measuring it. We'll also show it's importance in countless radio design problems. — *73! Eric*.

Build Your Go-Kit with DX Engineering!

DX ENGINEERING

Coaxial Cable Assemblies

These low-loss cable assemblies are available in standard lengths with DX Engineering's revolutionary patented PL-259 connector. Use the online Custom Cable Builder at DXEngineering.com to build assemblies made to your exact specs. DX Engineering's coaxial cable is also available by the foot or in bulk spools. **Enter "DXE Cable" at DXEngineering.com.**

---

iPortable · NANUK · GATOR Cases

Equipment Cases

Protect your sensitive equipment! DX Engineering boasts three rugged options to keep your gear safe: virtually indestructible Gator Equipment Rack Cases for transporting everything you need in your Go-Kit; high-impact resin NANUK cases now available in more size and color options, including units that perfectly fit RigExpert Antenna Analyzers; and iPortable units that combine a travel case with a DC power distribution point, speaker, and rack shelving. **Enter "Equipment Case" at DXEngineering.com.**

DC Outlet Panels and Battery Backup Systems

West Mountain RADIO

Bid farewell to that annoying tangle of spaghetti wire with RIGrunner DC outlet panels from West Mountain Radio. These outlets are fused for protection and ensure you have reliable power distribution. They provide 40 amps of maximum power and include from 4 to 12 Powerpole® connectors. West Mountain also makes backup devices, such as the Super PWRgate, which instantly switches to battery backup if you lose power. **Enter "West Mountain" at DXEngineering.com.**

ON ALL BANDS

DX Engineering's Amateur Radio Blog for New and Experienced Hams.

Visit OnAllBands.com for information you can use to improve your on-air experience.

ELECRAFT · DIAMOND ANTENNA · Palstar · DAIWA · MOONRAKER · AMERITRON · Coaxial Dynamics

SWR/Wattmeters

Measure forward and reflected transmitter power with SWR/wattmeters from top brands, including Ameritron, Coaxial Dynamics, Daiwa, Diamond, Elecraft, and Palstar. Choose from models with true peak and average readings, 20/200/2,000-watt ranges, amplifier bypass for high SWR, high SWR audio alarms, remote sensors, and more. Choose from two Daiwa Economy Series HF/VHF Bench Meter models (up to 200 watts or 1,500 watts maximum power). From Moonraker comes a range of new compact VSWR/power meters with power handling up to 400 watts. **Enter "Wattmeter" at DXEngineering.com.**

DX ENGINEERING · ICOM · COMET · AlexLoop · CHAMELEON ANTENNA

Portable Antennas

Need a versatile and easy-to-transport antenna? You'll find it here! Models include DX Engineering's EZ-BUILD UWA Center T and End Insulator Kits that let you build virtually any wire antenna type; Icom's 40-10M Magnetic Loop Antenna for the IC-705; a wide selection of rugged Comet HT and mobile antennas for upgraded performance; options from Chameleon, including the new 3.0 version of its F-Loop Portable Antennas, EMCOMM II and III HF antennas, and HF Backpack Antenna Systems; AlexLoop's HamPack Portable Magnetic Loop Antenna System; and many more. **Enter "Portable Antenna" at DXEngineering.com.**

ASTRON CORPORATION · YAESU · AMERITRON · KENWOOD · ALINCO · samlexamerica

Power Supplies

Make DX Engineering your source for reliable switching and linear power supplies from major brands, including Alinco, Ameritron, Astron, Samlex, Yaesu, and more. Choose from units with input voltages from 85 to 260 Vac and peak outputs from 10 to 50 amps. **Enter "Power Supplies" at DXEngineering.com.**

Tigertronics SignaLink™ USB Digital Communication Interface Packages

Tigertronics Grants Pass, Oregon

These combos pair a Tigertronics SignaLink USB with radio-specific interface cables for Alinco, Elecraft, Icom, Kenwood, Yaesu, and other rigs. Made for simple hookup to a Mac or PC, the SignaLink USB comes with a built-in low-noise sound card that supports all digital and voice modes, including WSJT. **Enter "Tigertronics" at DXEngineering.com.**

YAESU · ICOM · KENWOOD · ALINCO · HEIL HAM RADIO · RM ITALY · PRYME · GENERAC

Get Your Copy of Our New Catalog at DXEngineering.com!

DX® ENGINEERING

Ordering (via phone) Country Code: +1
9 am to midnight ET, Monday-Friday
9 am to 5 pm ET, Weekends

Phone or e-mail Tech Support: 330-572-3200
9 am to 7 pm ET, Monday-Friday
9 am to 5 pm ET, Saturday

Email: DXEngineering@DXEngineering.com

Ohio Showroom Hours:
9 am to 5 pm ET, Monday-Saturday

Ohio Curbside Pickup:
9 am to 8 pm ET, Monday-Saturday
9 am to 7 pm ET, Sunday

Nevada Curbside Pickup:
9 am to 7 pm PT, Monday-Sunday

800-777-0703 | DXEngineering.com

ON ALL BANDS · YouTube

We're All Elmers Here! Ask us at: Elmer@DXEngineering.com
Email Support 24/7/365 at DXEngineering@DXEngineering.com

Raising the bar on performance and reliability!

RECENT STEPPIR INNOVATIONS

1 NEW BRUSH/CONTACT ASSEMBLY

The new element housing unit (EHU) brush/contact assembly has greatly reduced friction buildup, with an average 36% friction reduction over the product life-cycle. The new assembly achieves this advantage without affecting product life expectations. The brush contact combination wears at a similar rate as our previous contacts. This new brush/contact not only has lower friction and the same longevity, it also greatly reduces RF noise during the tuning process due to the material properties of the contact.

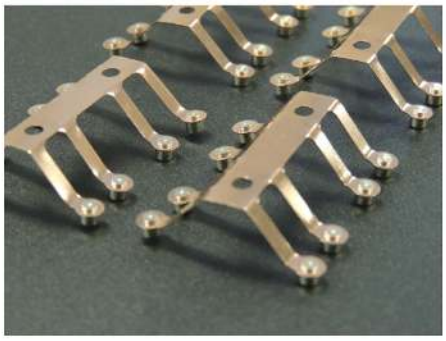

2 NEW COPPER STRIP INDEXING

The engineering team at SteppIR has completely redesigned our copper strip indexing and crowning system – this has taken the better part of a year of extensive design and testing, along with a near total reconfiguration of the system. The resulting improvement in accuracy, pitch and repeatability is now producing the most consistent and reliable material we have ever had.

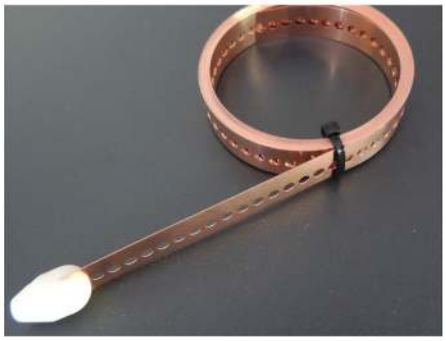

3 NEW 40/30 SWEEP ASSEMBLY

We always make it a point to listen closely to our customer base – we consider them to be an extension of our engineering department and are very thankful to have this resource. Thanks to a great initial idea we heard about from a few of our customers, we were able to leverage that knowledge into an all-new sweep system for our 40/30 loops. The new system will make the installation of antennas with loops, significantly easier and much more reliable. And, our new diverter system for the sweep return, will ensure that the copper conductor has a clear path through the sweep material at all times. This new design will eliminate the need for the sweep couplers.

steppIR COMMUNICATION SYSTEMS

20TH ANNIVERSARY steppIR

FOR PRODUCT DETAILS AND ORDERING:

www.steppir.com 425-453-1910